

© 2020 Elsevier. This manuscript version is made available under the CC-BY-NC-ND 4.0

# A comparative assessment of the performance of fungal-bacterial and fungal biofilters for methane abatement

**Alberto Vergara-Fernández<sup>1\*</sup>, Felipe Scott<sup>1</sup>, Felipe Carreño<sup>1</sup>, Germán Aroca<sup>2</sup>, Patricio Moreno-Casas<sup>1</sup>, Armando González-Sánchez<sup>3</sup> and Raúl Muñoz<sup>4</sup>**

<sup>1</sup> Green Technology Research Group, Facultad de Ingeniería y Ciencias Aplicadas, Universidad de los Andes, Chile.

<sup>2</sup> Escuela de Ingeniería Bioquímica, Facultad de Ingeniería, Pontificia Universidad Católica de Valparaíso. Chile

<sup>3</sup> Instituto de Ingeniería, Universidad Nacional Autónoma de México, Circuito Escolar, Ciudad Universitaria, 04510 Mexico City, Mexico

<sup>4</sup> Institute of Sustainable Processes, Universidad de Valladolid, Dr Mergelina s/n, 47011, Spain

\*Corresponding author: A. Vergara-Fernández. Tel.+ 562 2618 1441. E-mail: [aovergara@miuandes.cl](mailto:aovergara@miuandes.cl)

1  
2  
3  
4 **Abstract**  
5

6 Methane is an important contributor to global warming and especially for dilute emissions, its  
7 oxidation to carbon dioxide can be difficult and expensive. Biofiltration of streams carrying  
8 methane at low concentration in air have been treated with biofilters inoculated with  
9 methanotrophic bacteria. However, the role of fungi in methane is not well understood.  
10

11 In this work, methane abatement was studied in a biofilter inoculated solely with the filamentous  
12 fungus *Fusarium solani* and compared to a biofilter inoculated with a consortium of  
13 methanotrophic bacteria (*Methylomicrobium album* and *Methylocystis sp*) and *F. solani*.  
14

15 Results showed that *F. solani* degrade methane as the sole carbon source, achieving a maximum  
16 elimination capacity of 42.2 g m<sup>-3</sup> h<sup>-1</sup>, nearly half of the maximum elimination capacity of the  
17 fungal-bacterial consortium. Co-feeding o methane and *n*-pentane, a highly hydrophobic and easily  
18 degradable VOC, further improved the elimination capacity of both biofilters, with the elimination  
19 capacity of the fungal biofilter surpassing the one attained by the fungal-bacterial biofilter.  
20

21 A concise mathematical model of the biofilter together with the evaluation of the second  
22 Damköhler number indicated that under the operational conditions here applied, the fungal biofilter  
23 performance was bioreaction limited meanwhile external mass transport limitation was found on  
24 the fungal/methanotrophic bacteria biofilter.  
25

26 These results, and the estimated mass transfer coefficients, suggest that the beneficial effect of *F.*  
27 *solani* during CH<sub>4</sub> biofiltration was mediated by biomass hydrophobicity rather than to the  
28 formation of aerial hyphae structures increasing the mass transfer area.  
29

30  
31  
32  
33  
34  
35  
36  
37  
38  
39  
40  
41  
42  
43  
44  
45  
46  
47  
48  
49  
50  
51  
52  
53  
54  
55  
56  
57  
58  
59  
60  
61  
62  
63  
64  
65  
66  
67  
68  
69  
70  
71  
72  
73  
74  
75  
76  
77  
78  
79  
80  
81  
82  
83  
84  
85  
86  
87  
88  
89  
90  
91  
92  
93  
94  
95  
96  
97  
98  
99  
100  
101  
102  
103  
104  
105  
106  
107  
108  
109  
110  
111  
112  
113  
114  
115  
116  
117  
118  
119  
120  
121  
122  
123  
124  
125  
126  
127  
128  
129  
130  
131  
132  
133  
134  
135  
136  
137  
138  
139  
140  
141  
142  
143  
144  
145  
146  
147  
148  
149  
150  
151  
152  
153  
154  
155  
156  
157  
158  
159  
160  
161  
162  
163  
164  
165  
166  
167  
168  
169  
170  
171  
172  
173  
174  
175  
176  
177  
178  
179  
180  
181  
182  
183  
184  
185  
186  
187  
188  
189  
190  
191  
192  
193  
194  
195  
196  
197  
198  
199  
200  
201  
202  
203  
204  
205  
206  
207  
208  
209  
210  
211  
212  
213  
214  
215  
216  
217  
218  
219  
220  
221  
222  
223  
224  
225  
226  
227  
228  
229  
230  
231  
232  
233  
234  
235  
236  
237  
238  
239  
240  
241  
242  
243  
244  
245  
246  
247  
248  
249  
250  
251  
252  
253  
254  
255  
256  
257  
258  
259  
260  
261  
262  
263  
264  
265  
266  
267  
268  
269  
270  
271  
272  
273  
274  
275  
276  
277  
278  
279  
280  
281  
282  
283  
284  
285  
286  
287  
288  
289  
290  
291  
292  
293  
294  
295  
296  
297  
298  
299  
300  
301  
302  
303  
304  
305  
306  
307  
308  
309  
310  
311  
312  
313  
314  
315  
316  
317  
318  
319  
320  
321  
322  
323  
324  
325  
326  
327  
328  
329  
330  
331  
332  
333  
334  
335  
336  
337  
338  
339  
340  
341  
342  
343  
344  
345  
346  
347  
348  
349  
350  
351  
352  
353  
354  
355  
356  
357  
358  
359  
360  
361  
362  
363  
364  
365  
366  
367  
368  
369  
370  
371  
372  
373  
374  
375  
376  
377  
378  
379  
380  
381  
382  
383  
384  
385  
386  
387  
388  
389  
390  
391  
392  
393  
394  
395  
396  
397  
398  
399  
400  
401  
402  
403  
404  
405  
406  
407  
408  
409  
410  
411  
412  
413  
414  
415  
416  
417  
418  
419  
420  
421  
422  
423  
424  
425  
426  
427  
428  
429  
430  
431  
432  
433  
434  
435  
436  
437  
438  
439  
440  
441  
442  
443  
444  
445  
446  
447  
448  
449  
450  
451  
452  
453  
454  
455  
456  
457  
458  
459  
460  
461  
462  
463  
464  
465  
466  
467  
468  
469  
470  
471  
472  
473  
474  
475  
476  
477  
478  
479  
480  
481  
482  
483  
484  
485  
486  
487  
488  
489  
490  
491  
492  
493  
494  
495  
496  
497  
498  
499  
500  
501  
502  
503  
504  
505  
506  
507  
508  
509  
510  
511  
512  
513  
514  
515  
516  
517  
518  
519  
520  
521  
522  
523  
524  
525  
526  
527  
528  
529  
530  
531  
532  
533  
534  
535  
536  
537  
538  
539  
540  
541  
542  
543  
544  
545  
546  
547  
548  
549  
550  
551  
552  
553  
554  
555  
556  
557  
558  
559  
560  
561  
562  
563  
564  
565  
566  
567  
568  
569  
570  
571  
572  
573  
574  
575  
576  
577  
578  
579  
580  
581  
582  
583  
584  
585  
586  
587  
588  
589  
590  
591  
592  
593  
594  
595  
596  
597  
598  
599  
600  
601  
602  
603  
604  
605  
606  
607  
608  
609  
610  
611  
612  
613  
614  
615  
616  
617  
618  
619  
620  
621  
622  
623  
624  
625  
626  
627  
628  
629  
630  
631  
632  
633  
634  
635  
636  
637  
638  
639  
640  
641  
642  
643  
644  
645  
646  
647  
648  
649  
650  
651  
652  
653  
654  
655  
656  
657  
658  
659  
660  
661  
662  
663  
664  
665  
666  
667  
668  
669  
670  
671  
672  
673  
674  
675  
676  
677  
678  
679  
680  
681  
682  
683  
684  
685  
686  
687  
688  
689  
690  
691  
692  
693  
694  
695  
696  
697  
698  
699  
700  
701  
702  
703  
704  
705  
706  
707  
708  
709  
710  
711  
712  
713  
714  
715  
716  
717  
718  
719  
720  
721  
722  
723  
724  
725  
726  
727  
728  
729  
730  
731  
732  
733  
734  
735  
736  
737  
738  
739  
740  
741  
742  
743  
744  
745  
746  
747  
748  
749  
750  
751  
752  
753  
754  
755  
756  
757  
758  
759  
760  
761  
762  
763  
764  
765  
766  
767  
768  
769  
770  
771  
772  
773  
774  
775  
776  
777  
778  
779  
780  
781  
782  
783  
784  
785  
786  
787  
788  
789  
790  
791  
792  
793  
794  
795  
796  
797  
798  
799  
800  
801  
802  
803  
804  
805  
806  
807  
808  
809  
810  
811  
812  
813  
814  
815  
816  
817  
818  
819  
820  
821  
822  
823  
824  
825  
826  
827  
828  
829  
830  
831  
832  
833  
834  
835  
836  
837  
838  
839  
840  
841  
842  
843  
844  
845  
846  
847  
848  
849  
850  
851  
852  
853  
854  
855  
856  
857  
858  
859  
860  
861  
862  
863  
864  
865  
866  
867  
868  
869  
870  
871  
872  
873  
874  
875  
876  
877  
878  
879  
880  
881  
882  
883  
884  
885  
886  
887  
888  
889  
890  
891  
892  
893  
894  
895  
896  
897  
898  
899  
900  
901  
902  
903  
904  
905  
906  
907  
908  
909  
910  
911  
912  
913  
914  
915  
916  
917  
918  
919  
920  
921  
922  
923  
924  
925  
926  
927  
928  
929  
930  
931  
932  
933  
934  
935  
936  
937  
938  
939  
940  
941  
942  
943  
944  
945  
946  
947  
948  
949  
950  
951  
952  
953  
954  
955  
956  
957  
958  
959  
960  
961  
962  
963  
964  
965  
966  
967  
968  
969  
970  
971  
972  
973  
974  
975  
976  
977  
978  
979  
980  
981  
982  
983  
984  
985  
986  
987  
988  
989  
990  
991  
992  
993  
994  
995  
996  
997  
998  
999  
1000

Keywords: Methane abatement; *Fusarium solani*; Biofiltration; Mass transfer coefficient;  
Mathematical modeling.

## 1 Introduction

Methane (CH<sub>4</sub>) is considered as a relevant greenhouse gas since its contribution to global warming in a 100 y horizon accounts for ~ 23%, while carbon dioxide (CO<sub>2</sub>) contributes to 70%. Besides CH<sub>4</sub> has an average global warming potential 28 (in a 100 y horizon) times higher than CO<sub>2</sub> [1]. Atmospheric CH<sub>4</sub> concentration is increasing twice faster than CO<sub>2</sub> concentration [2,3].

In this context, biofiltration is a cost-effective alternative to control off-gas emissions of CH<sub>4</sub> below the flammability point (5% v/v)[2,4]. Indeed, methanotrophs-based biofilters have been extensively applied during the past two decades to reduce CH<sub>4</sub> emissions from landfills, livestock farms or even coal mines [5]. However, the low aqueous solubility of CH<sub>4</sub> (dimensionless gas-liquid Henry's law constant of 29.4 at 1 atm and 25°C) limits its cost-effective biological abatement [3]. Biofiltration systems typically contain mixed microbial populations (i.e. bacteria, fungi and yeasts) adapted to oxidize particular pollutants under ambient conditions (pH, temperature, moisture content, etc.). The use of fungi in biofilters may offer several advantages compared to conventional bacteria colonized-biofilters, such as a higher enzyme diversity and tolerance to extremophile conditions (low nutrient availability, low water activity and low pH values) [6]. In addition, several authors have claimed that the empty bed fraction of biofilters can be colonized by aerial hyphae. This can enhance the elimination capacity of hydrophobic pollutants such as CH<sub>4</sub> based on the increase in the specific mass transfer area mediated by hyphae growth, which are covered by lyophilic proteins able to easily solubilize hydrophobic gases [7–9]. In this context, the co-culture of filamentous fungi with methanotrophic bacteria can increase the CH<sub>4</sub> elimination capacity by increasing the partition coefficient of CH<sub>4</sub> in the biofilm established in the biofilter packed bed (bioavailability) [10,11].

1  
2  
3  
4 The potential of fungi as a biological platform for enhancing the availability and biodegradation of  
5  
6 methane has been reported by several authors [11–14]. Girard et al. [12] inoculated the fungi  
7  
8 *Candida ingens*, *Sporotrichum pruinosum*, *Coprinus sp.* and *Cunninghamella elegans* in  
9  
10 combination with methanotrophic bacteria in a biofilter treating methane, reaching a maximum  
11  
12 methane elimination capacity (EC) of  $18.8 \text{ g m}^{-3} \text{ h}^{-1}$  at an inlet load of  $46.7 \text{ g m}^{-3} \text{ h}^{-1}$ . Lebrero et  
13  
14 al. (2016) reported that *Graphium sp.* was able to degrade methane only when methanol was  
15  
16 supplemented as a co-substrate. These authors evaluated also the performance and microbiology  
17  
18 of a fungal-bacterial compost biofilter treating methane concentrations of 2% at empty bed  
19  
20 residence times of 40 and 20 min under different irrigation rates, with daily mineral medium  
21  
22 addition of 200 mL supporting EC of  $37 \text{ g m}^{-3} \text{ h}^{-1}$ . Recently, Vergara-Fernández et al. [11] reported  
23  
24 the ability of *Fusarium solani* to biodegrade  $\text{CH}_4$  as the sole carbon source in microcosm  
25  
26 experiments ( $0.3 \text{ g m}^{-3} \text{ h}^{-1}$  at  $35^\circ\text{C}$  and water activity of 0.95). To our understanding, this was the  
27  
28 first report of methane consumption by fungi as the sole carbon and energy source. Moreover, *F.*  
29  
30 *solani* could decrease the partition coefficient of methane up to two orders of magnitude compared  
31  
32 with the partition coefficient of methane in water.  
33  
34  
35  
36  
37  
38  
39  
40  
41  
42

43 Mathematical modelling represents a powerful tool to optimize the design and operation of  
44  
45 biological gas-treatment units. In this context, several reactive-internal transport/external transport  
46  
47 based mathematical models have been reported to describe  $\text{CH}_4$  oxidation in biofilters inoculated  
48  
49 with methanotrophic bacteria under isothermal conditions [15,16] and under non-isothermal  
50  
51 conditions [17]. However, to our knowledge, mathematical models describing fungi-based methane  
52  
53 biofilters are scarce, which limits the developments of these high-performance biofilters.  
54  
55  
56  
57  
58  
59  
60  
61  
62  
63  
64  
65

1  
2  
3  
4 This work aims at characterizing for the first time the effects of CH<sub>4</sub> inlet load and residence time,  
5  
6 as well as *n*-pentane co-feeding, on the performance of a biofilter treating methane using the fungi  
7  
8 *Fusarium solani* alone and in a consortium with methanotrophic bacteria. Secondly, the role of the  
9  
10 fungal biomass as an enhancer of methane bioavailability in the biofilms was explored, both  
11  
12 experimentally and through a mathematical model.  
13  
14  
15  
16  
17  
18

## 19 **2 Materials and methods**

### 20 21 2.2 Microorganisms and inoculum

22  
23 The methanotrophic bacteria used in this work were *Methylobacterium album* ATCC 33003 and  
24  
25 *Methylocystis* sp. ATCC 4924. Bacterial propagation was performed in NMS (Nitrate-mineral salt  
26  
27 medium, ATCC 1306) without agar at pH 6.8 as previously reported by Cáceres et al. [18].  
28  
29 Propagation of the filamentous fungi *Fusarium solani* B1 (CBS 117476) was carried out as  
30  
31 described by Morales et al. [19] in potato-dextrose agar. Fungal preservation, cultivation conditions  
32  
33 and spore production were similar to those reported by García-Peña et al. [20]. Cultures were  
34  
35 incubated in a rotary shaker (Incu-Shaker Mini, Benchmark) at 30°C and 80 or 200 rpm for fungi  
36  
37 and bacteria cultivation, respectively.  
38  
39  
40  
41  
42  
43  
44

### 45 2.3 Carbon source and mineral medium

46  
47 The carbon sources used as model hydrophobic contaminants in the different experiments were  
48  
49 methane (Indura Chile, 99.99%) and *n*-pentane (Merck, 99%). Glycerol (Merck, 99.9%) and  
50  
51 methanol (Merck, 99.9%) were used as alternative carbon sources to support microbial growth  
52  
53 during the start-up period of the biofilters. The mineral salt medium used for fungal growth in  
54  
55 liquid cultures and biofiltration columns was previously reported by Arriaga and Revah (2005):  
56  
57 NaNO<sub>3</sub> 18 g L<sup>-1</sup>, KH<sub>2</sub>PO<sub>4</sub> 1.3 g L<sup>-1</sup>, MgSO<sub>4</sub>·7H<sub>2</sub>O 0.38 g L<sup>-1</sup>, CaSO<sub>4</sub>·2H<sub>2</sub>O 0.25 g L<sup>-1</sup>, CaCl<sub>2</sub> 0.055  
58  
59  
60  
61  
62  
63  
64  
65

1  
2  
3  
4 g L<sup>-1</sup>, FeSO<sub>4</sub>·7H<sub>2</sub>O 0.015 g L<sup>-1</sup>, MnSO<sub>4</sub>·H<sub>2</sub>O 0.012 g L<sup>-1</sup>, ZnSO<sub>4</sub>·7H<sub>2</sub>O 0.013 g L<sup>-1</sup>, CuSO<sub>4</sub>·7H<sub>2</sub>O  
5  
6 0.0023 g L<sup>-1</sup>, CoCl<sub>2</sub>·6H<sub>2</sub>O 0.0015 g L<sup>-1</sup>, H<sub>3</sub>BO<sub>3</sub> 0.0015 g L<sup>-1</sup> and glycerol 10 mL L<sup>-1</sup>.  
7  
8

9 The composition of NMS medium used for bacterial growth was as follows [22]: MgSO<sub>4</sub>·7H<sub>2</sub>O  
10  
11 1.0 g L<sup>-1</sup>, CaCl<sub>2</sub>·6H<sub>2</sub>O 0.2 g L<sup>-1</sup>, KNO<sub>3</sub> 1.0 g L<sup>-1</sup>, KH<sub>2</sub>PO<sub>4</sub> 0.272 g L<sup>-1</sup>, Na<sub>2</sub>HPO<sub>4</sub>·12H<sub>2</sub>O 0.717 g  
12  
13 L<sup>-1</sup>, 2.0 mL of chelated iron and 0.5 mL of a trace elements solution was additionally added to 1 L  
14  
15 of NMS solution. The chelated iron solution contains: 1.0 g L<sup>-1</sup> ferric (III) ammonium citrate, 2.0  
16  
17 g L<sup>-1</sup> EDTA sodium salt, 0.3 mL of HCl (concentrated), 100 mL of distilled deionized water. The  
18  
19 trace element solution contains per liter of distilled water: EDTA 0.5 g L<sup>-1</sup>, FeSO<sub>4</sub>·7H<sub>2</sub>O 0.2 g L<sup>-1</sup>,  
20  
21 ZnSO<sub>4</sub>·7H<sub>2</sub>O 0.01 g L<sup>-1</sup>, MnCl<sub>2</sub>·4H<sub>2</sub>O 0.003 g L<sup>-1</sup>, H<sub>3</sub>BO<sub>3</sub> 0.03 g L<sup>-1</sup>, CoCl<sub>2</sub>·6H<sub>2</sub>O 0.02 g L<sup>-1</sup>,  
22  
23 CaCl<sub>2</sub>·2H<sub>2</sub>O 0.001 g L<sup>-1</sup>, NiCl<sub>2</sub>·6H<sub>2</sub>O 0.002 g L<sup>-1</sup>, Na<sub>2</sub>MoO<sub>4</sub>·2H<sub>2</sub>O 0.003 g L<sup>-1</sup>.  
24  
25  
26  
27  
28  
29  
30

#### 31 *2.4 Experimental set-up for methane biofiltration*

32

33 A diagram of the experimental system is shown in Figure 1. Two identical biofilters were set up  
34  
35 with PVC-clear columns (7.9 cm of diameter and 105 cm of height) divided into three equal length  
36  
37 modules. Each module was filled with 82 g of vermiculite (empty bed  $\epsilon$  of 69%), reaching a total  
38  
39 packed bed volume ( $V_p$ ) of 2.35 L. Each module was periodically sampled at the inlet and the outlet  
40  
41 of the gaseous stream from sampling ports. The moisture content of the solid support and the  
42  
43 pressure drop in each module of the biofilter were determined with a ProCheck sensor read-out  
44  
45 device (Decagon Devices, WA, USA) and a U-Tube manometer (using water as the manometric  
46  
47 fluid), respectively. The moisture content in the airstream at the inlet and the outlet of biofilter were  
48  
49 measured with a thermo-hygrometer (Testo 625, Testo, PA, USA). The biofilters were  
50  
51 continuously fed with different mixtures of pre-humidified air and pure CH<sub>4</sub> (99.99%, Indura  
52  
53 Chile). The humidifier consisted of a PVC-Clear column (diameter of 7.9 cm and 40 cm height)  
54  
55  
56  
57  
58  
59  
60  
61  
62  
63  
64  
65

filled with 20 cm of water.

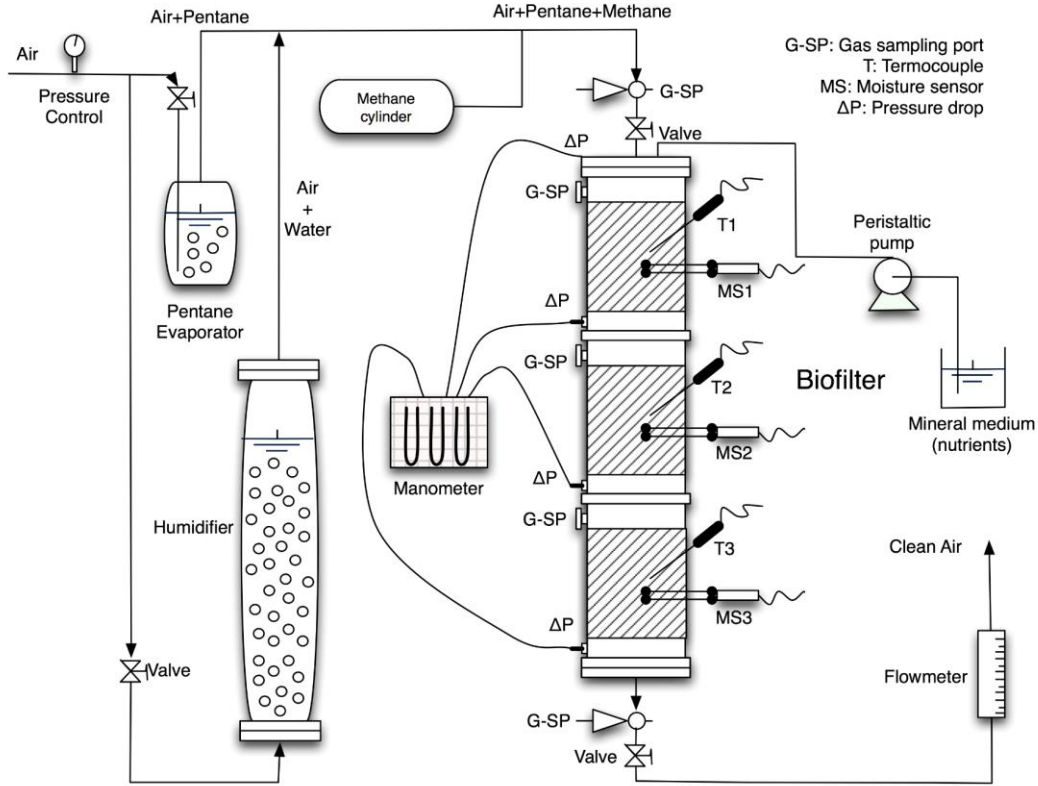


**Figure 1.** Schematic diagram of the laboratory-scale biofilter system

The performance of the methane biofilters was expressed in terms of methane elimination capacity ( $EC$ ,  $\text{g CH}_4 \text{ m}^{-3} \text{ h}^{-1}$ ), and methane and  $n$ -pentane inlet loading rate ( $IL$ ,  $\text{g m}^{-3} \text{ h}^{-1}$ ), which were correlated with the empty bed residence time (EBRT):

$$EBRT = \frac{V_p}{Q} \quad (1)$$

$$EC = \frac{(C_{g,0} - C_{g,out})}{EBRT} \quad (2)$$

$$IL = \frac{(C_{g,0})}{EBRT} \quad (3)$$

Where  $Q$  and  $V_p$  represent the polluted air flow rate ( $\text{m}^3 \text{ h}^{-1}$ ) and packed bed volume ( $\text{m}^3$ ), respectively,  $C_{g,0}$  and  $C_{g,out}$  the inlet and outlet methane concentrations ( $\text{g m}^{-3}$ ) in the polluted

1  
2  
3  
4 airflow, respectively.  
5

6  
7 The study of the influence of CH<sub>4</sub> inlet load on biofilters performance was conducted by setting  
8  
9 different concentrations of CH<sub>4</sub> adjusting the flow rate of pure methane and humidified air. Both  
10  
11 flow rates were controlled with mass flow controllers (Colepalmer, EW-32907-69, IL, USA). In  
12  
13 the experiments where *n*-pentane or methanol were used, a stream of air controlled with a mass  
14  
15 flow controller (Colepalmer, EW-32907-69, IL, USA) was bubbled in an evaporator with *n*-  
16  
17 pentane or with methanol (depending on the experimental stage), and subsequently mixed with a  
18  
19 humidied air stream containing methane  
20  
21  
22

## 23 24 25 26 2.5 Operational strategies during CH<sub>4</sub> biofiltration 27

28 The two biofilters were operated in parallel. The fungal biofilter (BF) was inoculated with the  
29  
30 fungus *F. solani*, while the Fungal-Bacterial Biofilter (FBB) was inoculated with a methanotrophic  
31  
32 bacterial consortium composed of *Methylomicrobium album* and *Methylocystis* sp., and the fungus  
33  
34 *F. solani*. All microorganisms used were previously grown in their respective mineral medium and  
35  
36 glycerol at 4 g L<sup>-1</sup>.  
37

38  
39  
40 BF was inoculated with a mixture of 1000 mL of fungi (2.0 g L<sup>-1</sup>) in mineral medium and 400 mL  
41  
42 of fresh mineral medium, which was recirculated for 7 days through the packed column to favor  
43  
44 the attachment of the microorganisms. FBB was inoculated with a mixture of 500 mL of  
45  
46 methanotrophic bacterial culture (1.0 g L<sup>-1</sup>) and 500 mL of fungal culture (2.0 g L<sup>-1</sup>). The cell  
47  
48 suspension containing both fungi and bacteria was mixed with 400 mL of mineral medium and  
49  
50 recirculated for 7 days through the packed column to allow the attachment of the microorganisms.  
51  
52

53  
54 A methane laden airstream was fed to the columns for 80 days at an inlet concentration of 25 g  
55  
56 CH<sub>4</sub> m<sup>-3</sup> and a gas flow of 0.181 L min<sup>-1</sup> (EBRT equal to 13 min), corresponding to an inlet load  
57  
58 of 115.4 ±5.2 g m<sup>-3</sup> h<sup>-1</sup>. Methanol at a concentration of 1.0 g m<sup>-3</sup> was supplemented to the CH<sub>4</sub>-  
59  
60  
61

1  
2  
3  
4 laden emission from day 33 to 40 according to Lebrero et al. [13] in order to foster microbial  
5  
6 growth and CH<sub>4</sub> biodegradation in the biofilters. At day 55, 100 mL of mineral salt medium with  
7  
8 glycerol at 4 g L<sup>-1</sup> was added to the biofilters according to Vergara-Fernández et al. [23] while  
9  
10 maintaining the methane inlet load.  
11  
12  
13  
14

### 15 16 2.5.1 *Influence of CH<sub>4</sub> loading rate and EBRT on the steady-state CH<sub>4</sub> elimination capacity*

17  
18 The influence of the methane loading rate on the elimination capacity of FB and FBB was assessed  
19  
20 by increasing the inlet CH<sub>4</sub> concentration from 6 to 94 g CH<sub>4</sub> m<sup>-3</sup> at a constant *EBRT* of 12.2 (±0.9)  
21  
22 min, which corresponded to loading rates between 31.6 and 437 g CH<sub>4</sub> m<sup>-3</sup> h<sup>-1</sup>. On the other hand,  
23  
24 the influence of the *EBRT* on the methane elimination capacity was assessed by varying the *EBRT*  
25  
26 between 6.0 and 23.3 min at a constant methane inlet load of 437(±5.9) g CH<sub>4</sub> m<sup>-3</sup> h<sup>-1</sup>.  
27  
28  
29  
30  
31  
32

### 33 2.5.2 *Influence of n-pentane supplementation on the CH<sub>4</sub> elimination capacity*

34  
35 The influence of *n*-pentane on the methane elimination capacity was evaluated by supplying *n*-  
36  
37 pentane loading rates ranging from 48.1 (±2.6) to 238.1 (±6.8) g *n*-pentane m<sup>-3</sup> h<sup>-1</sup> at a constant  
38  
39 methane loading rate of 131.1 (±5.0) g CH<sub>4</sub> m<sup>-3</sup> h<sup>-1</sup>.  
40  
41  
42  
43  
44

## 45 2.6 *Estimation of Fusarium solani contribution to CH<sub>4</sub> biodegradation*

46  
47 Methane biodegradation tests in microcosms were performed in order to quantify the contribution  
48  
49 of *Fusarium solani* towards the methane elimination in the biofilter. Samples of 2.0 g of vermiculite  
50  
51 with biomass were withdrawn from the biofilters FB and FBB by day 80. The samples were mixed  
52  
53 with 10 mL of mineral medium containing the antifungal amphotericin B at a concentration of 32  
54  
55 µg mL<sup>-1</sup>. Control experiments without the addition of amphotericin B were also performed. The  
56  
57 consumption of methane as the sole carbon and energy source was assayed at an initial  
58  
59  
60  
61  
62  
63  
64  
65

concentration of 27 ( $\pm 1.5$ ) g m<sup>-3</sup> and 30°C for 15 days without stirring. The microcosms were established in 125 mL bottles hermetically sealed with 20 mm × 3 mm laminated silicone-PTFE (0.13 mm) septa, and aluminum seals.

## 2.7 K<sub>BA</sub> and Damköhler number estimation in biofilters treating CH<sub>4</sub>.

To determine the mechanism limiting CH<sub>4</sub> elimination in FBB and FB, the second Damköhler number (eq. 4) was calculated under the corresponding operational conditions, assuming that the fungal-bacterial biofilm and fungal biofilm followed first-order kinetics and Monod type kinetics, respectively (see supplementary section). This dimensionless number defines the ratio between the maximum methane biodegradation rate and the maximum methane mass transfer rate for a given condition. A second Damköhler number higher than one indicates the occurrence of external mass transfer limitation in the biofilter, while values lower than one are encountered in bioreaction limited scenarios [24].

$$Da_{II}^j = \begin{cases} \frac{k_X^j V_b^j}{K_B a^j (1-\epsilon) V_p}, & \text{for } j = FBB \\ \frac{q_{max} X_b^j V_b^j H^j}{K_B a^j (1-\epsilon) V_p} \cdot \frac{1}{C_g^{in}}, & \text{for } j = FB \end{cases} \quad \text{Eq. 4}$$

A series of experiments were carried out in order to estimate the overall mass transfer coefficient based on the biofilm phase (K<sub>BA</sub>) for both biofilters and the corresponding biokinetic parameters of the fungal or fungal-bacterial biofilm. The experiments were carried out at three different flows rates (0.3, 0.6 and 0.86 L min<sup>-1</sup>). CH<sub>4</sub> inlet concentrations of 19, 16.5 and 15.5 g CH<sub>4</sub> m<sup>-3</sup> were used in the FB tests, while CH<sub>4</sub> inlet concentrations of 28, 25 and 24 g CH<sub>4</sub> m<sup>-3</sup> were used in FBB. All experiments were performed at 30 °C. The experimental procedure was as follows: Under

1  
2  
3  
4 steady-state at the target inlet CH<sub>4</sub> concentration, the flow of pure CH<sub>4</sub> was interrupted until the  
5  
6 outlet air stream reached a CH<sub>4</sub> concentration equal to zero. Then, CH<sub>4</sub> supply was restored.

7  
8  
9 CH<sub>4</sub> concentration was quantified off-line by gas chromatography (see Analytical methods) at the  
10  
11 outlet of the biofilters. The time course and profiles of CH<sub>4</sub> concentrations were adjusted to a  
12  
13 comprehensive biofiltration mathematical model adapted from [25] (see supplementary material).  
14  
15

## 16 17 18 19 2.8 Analytical methods

20  
21 CH<sub>4</sub> gas concentration was determined from gas samples extracted using a 500 µL gas syringe  
22  
23 (Hamilton). The samples were injected in a gas chromatograph (Shimadzu 2014) equipped with a  
24  
25 TCD detector and a 60/80 Carboxen column (15 ft × 1/8 in × 2.1 mm). Injector temperature was  
26  
27 maintained at 150°C, while oven and detector temperatures were kept at 200°C and 220°C,  
28  
29 respectively. *n*-pentane gas concentration was measured by FID-GC in a Shimadzu 2014  
30  
31 chromatograph (detection temperature 220 °C, injection temperature 80 °C and column temperature  
32  
33 200 °C) equipped with a capillary column RTX-5 Restex UE (30 m × 0.32 mm × 0.25 µm), using  
34  
35 helium as a gas carrier.  
36  
37  
38  
39  
40  
41  
42  
43

## 44 2.9 Scanning electron microscope

45  
46 Samples of the vermiculite support with microbial consortium grown for 8 months were dried at  
47  
48 105 °C for 24 hours for scanning electron microscopy (SEM) imaging. Dried samples were  
49  
50 mounted onto stubs and gold-coated using JEOL fine-coat ion sputter JFC-1100. Samples were  
51  
52 visualized and micrographed using a scanning electron microscope (EVO MA 10 model, Zeiss),  
53  
54 with an EDS Penta FET Precision detector (Oxford Instruments X-act) at 20 kV accelerating  
55  
56  
57  
58  
59 voltage.  
60  
61  
62  
63  
64  
65

### 3 Results and discussion

#### 3.1 Biofilter start-up

The elimination capacities achieved in the biofilters during the first 80 days of operation are shown in Figure 2. During the first 20 days, both biofilters showed comparable EC, with average values of  $6.6(\pm 2.2) \text{ g m}^{-3} \text{ h}^{-1}$ . After 20 days of operation, an increase in the  $\text{CH}_4$  EC of FBB was recorded, reaching a stable average EC of  $17.5 \text{ g m}^{-3} \text{ h}^{-1}$ . Similar EC values were achieved in FB after 26 days of operation. This delay could be attributed to the slower growth rate of fungi compared to bacteria. Interestingly, both biofilters experienced a decrease in the EC after 30 days of operation, reaching values close to  $8.7 \text{ g m}^{-3} \text{ h}^{-1}$ . The reason underlying the observed decrease in EC were not clear since temperature and humidity remained constant at the set points, and mineral medium was added once per week. Methanol was fed at a loading rate of  $4.8 \text{ g m}^{-3} \text{ h}^{-1}$  from day 34 until day 55 in an attempt to increase the biomass content in the biofilters. This allowed increasing the  $\text{CH}_4$ -EC by 40% compared to the previous condition. 100 mL of mineral medium with  $4 \text{ g L}^{-1}$  glycerol were added at the end of day 55 to increase of biomass content in the biofilters. Figure 2 shows a rapid increase in EC in both biofilters following glycerol addition, reaching a maximum of  $32.8 \text{ g m}^{-3} \text{ h}^{-1}$  by day 60 and stabilizing at  $28.4(\pm 2.2) \text{ g m}^{-3} \text{ h}^{-1}$  in FBB. An average EC of  $21.8 \text{ g m}^{-3} \text{ h}^{-1}$  was achieved in BF from days 63 to 80. The increase in  $\text{CH}_4$  EC for both biofilters was likely due to the effectiveness of glycerol supporting a rapid growth of *F. solani* (*F. solani* was routinely grown in glycerol as sole carbon and energy source in our laboratory) in the biofilters. No growth enhancement was expected for the obligate methanotroph *Methylomicrobium album* ATCC 33003 [26] or the facultative methanotroph (able to grow on acetate and ethanol) *Methylocystis* sp. ATCC 4924 [27]. From day 80 onwards, the biofilters were operated with methane as the sole carbon and energy source (Figures 4, 5).

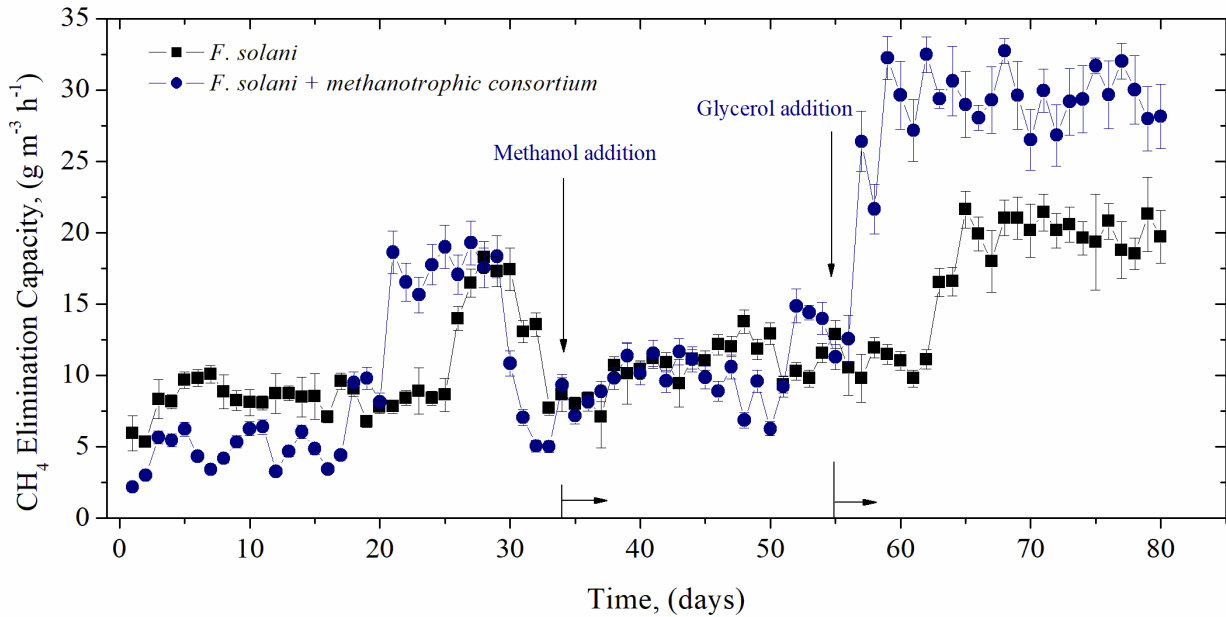


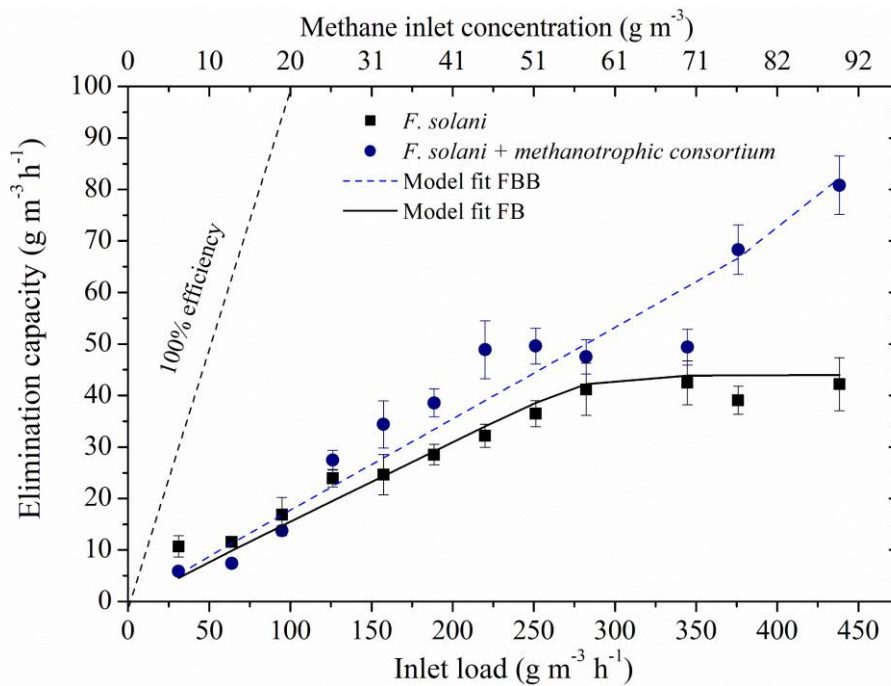
**Figure 2.** Time course of the methane elimination capacity of the biofilter inoculated solely with *Fusarium solani* and the biofilter inoculated with *Fusarium solani* and the methanotrophic consortium and operated at an inlet concentration of  $25 \text{ g CH}_4 \text{ m}^{-3}$  and *EBRT* 13 min, corresponding to  $115.4(\pm 5.2) \text{ g m}^{-3} \text{ h}^{-1}$ .

The maximum removal efficiencies recorded in FBB and FB were 26% and 17%, respectively, with EC comparable to those reported by Lebrero et al. [13] for a fungal-bacterial biofilter ( $35 \text{ g m}^{-3} \text{ h}^{-1}$ ). The EC achieved in this work was higher than the  $16 \text{ g m}^{-3} \text{ h}^{-1}$  attained by Pratt et al. [28] in a biofilter inoculated solely with a methanotrophic bacterial consortium.

### 3.2 Influence of $\text{CH}_4$ loading rate on the $\text{CH}_4$ elimination capacity

Figure 3 shows the  $\text{CH}_4$  EC recorded at the different methane loading rates applied in both biofilters. The results obtained for FB showed a methane EC of  $17 \text{ g m}^{-3} \text{ h}^{-1}$  for a critical methane loading rate of  $125 \text{ g m}^{-3} \text{ h}^{-1}$ . On the other hand, it was not possible to obtain the critical methane-

loading rate for FBB. CH<sub>4</sub> EC of 75 and 37 g m<sup>-3</sup> h<sup>-1</sup> were recorded in FBB and FB, respectively, at the maximum methane loading rate applied 450 g m<sup>-3</sup> h<sup>-1</sup>. The ECs at a loading rate of 125 g m<sup>-3</sup> h<sup>-1</sup> in FB and FBB were more than two times higher than the values reported by López et al. [29] for a loading rate of 120 g m<sup>-3</sup> h<sup>-1</sup> (11.3 g m<sup>-3</sup> h<sup>-1</sup>). Lebrero et al. [13] reported an EC of 70 g m<sup>-3</sup> h<sup>-1</sup> for a methane loading rate of 120 g m<sup>-3</sup> h<sup>-1</sup> in a bacterial-fungal biofilter inoculated with *Graphium* sp. However, these authors reported that *Graphium* sp. was eventually displaced from the biofilter community and that the fungus was able to use methane only when methanol was also present. The higher EC obtained in the FBB operated in this study may be explained by the increase in the interfacial gas-biofilm contact area due to the presence of the filaments from fungi [30] and by the increase in the CH<sub>4</sub> concentration gradient mediated by the hydrophobic properties of the fungal filaments [11,31]. These fungal mediated mechanisms could increase the bioavailability of methane in the whole methanotrophic biofilm, which ultimately supported higher CH<sub>4</sub> degradation rates [14]. The later highlights the advantage of deploying methanotrophic fungal/bacterial consortia during CH<sub>4</sub> biofiltration[11].



1  
2  
3  
4 **Figure 3.** Methane elimination capacity vs loading rates for the biofilter inoculated with *F. solani*  
5 (FB) and biofilter inoculated with *F. solani* and a methanotrophic bacteria consortium (FBB).  
6  
7  
8  
9 Model fits correspond to the solution of Eqs. S1-S3 with parameters shown in Table 1.  
10

### 11 12 13 14 3.3 Influence of the EBRT at constant CH<sub>4</sub> loading rate on the elimination capacity

15  
16 Figure 4 shows the effect of the EBRT at a CH<sub>4</sub> loading rate of 437(±5.9) g m<sup>-3</sup> h<sup>-1</sup> in the EC of FB  
17 and FBB. A decrease in CH<sub>4</sub> EC was observed at increasing gas flow rates in both biofilters, which  
18 can be explained by the shorter contact time between methane and the methanotrophic biofilm at  
19 lower EBRT. The main decrease in CH<sub>4</sub> EC in both biofilters was observed when the EBRT was  
20 reduced from 23.3 to 6.0 min, the greatest reduction being observed in FBB (13.4 g m<sup>-3</sup> h<sup>-1</sup>  
21 decrease) in comparison with the FB (7.4 g m<sup>-3</sup> h<sup>-1</sup> decrease). When both biofilters were operated  
22 at EBRTs between 26 and 13 min, the EC stabilized between 26 and 16 g m<sup>-3</sup> h<sup>-1</sup> in FBB and FB,  
23 respectively. Despite FBB supported the highest EC, its performance was severely affected by  
24 shorter EBRTs. This may be related to either the microbial structure, the morphology of the  
25 methanotrophic biofilm, or a combination of both. Bacterial population in the biofilm exhibited a  
26 low methane mass transfer capacity, which might explain the mass transfer limitations recorded  
27 under low EBRTs in FBB. This lower methane mass transfer capacity of methanotrophic bacteria  
28 was recently reported by Vergara-Fernández et al. [11] during the assessment of the partition  
29 coefficients of methane in *Fusarium solani* and methanotrophic bacteria biomass ( $C_g/C_{\text{biofilm}}$  of  
30 0.2631 and 2.192, respectively) under similar operational conditions than those used in the present  
31 study. On the other hand, the decrease in EBRT in FB entailed a less severe effect on CH<sub>4</sub> EC,  
32 which may be related to the more homogenous hyphae biofilm growth. Thus, a decrease in EBRT  
33 would exert less impact on CH<sub>4</sub> EC in a scenario of enhanced CH<sub>4</sub> concentration gradients  
34 mediated by fungal hydrophobicity (Vergara-Fernández et al., 2016).  
35  
36  
37  
38  
39  
40  
41  
42  
43  
44  
45  
46  
47  
48  
49  
50  
51  
52  
53  
54  
55  
56  
57  
58  
59  
60  
61  
62  
63  
64  
65

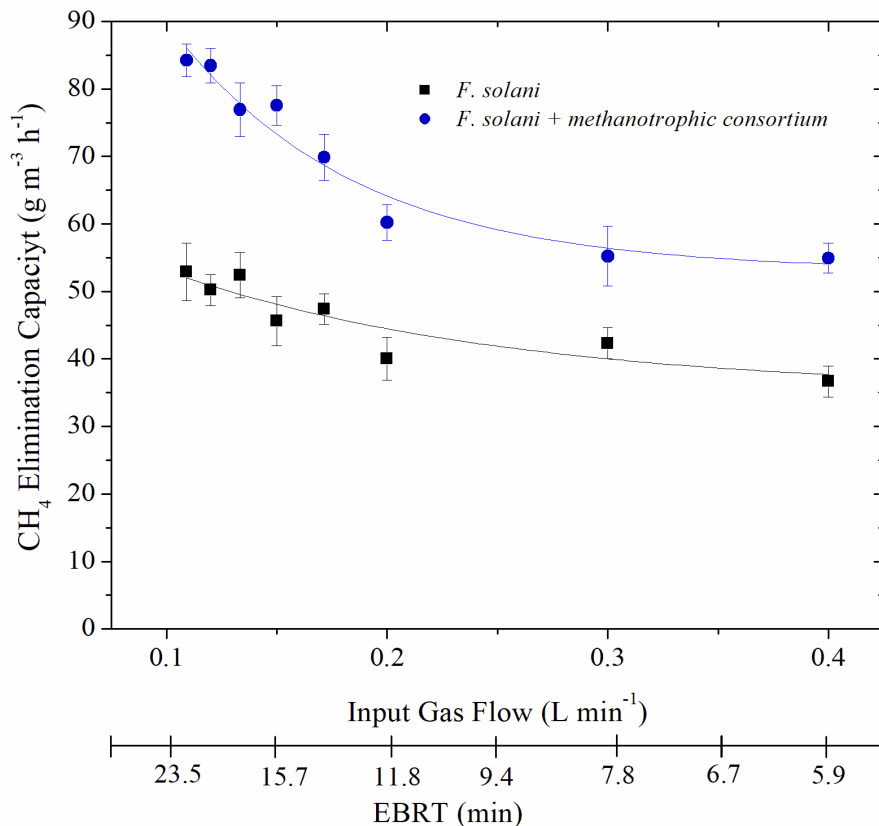
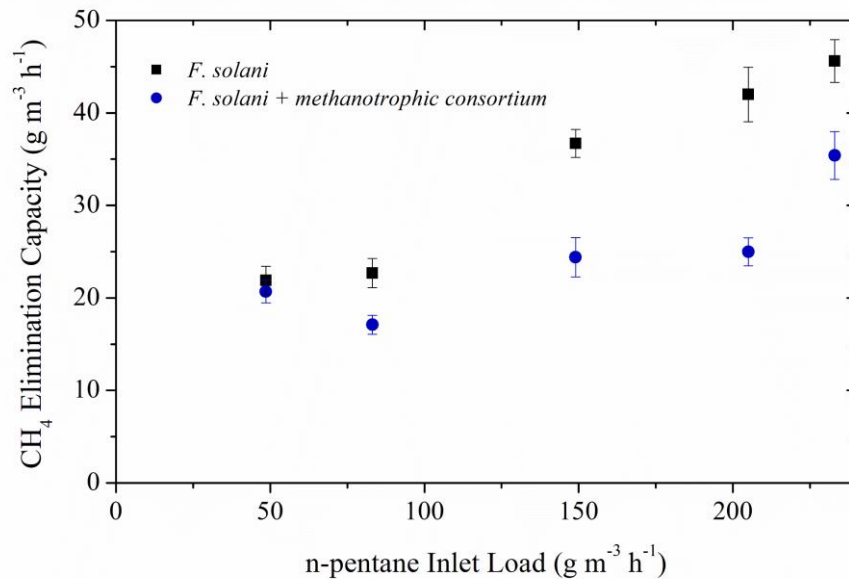


**Figure 4.** Influence of the *EBRT* on  $\text{CH}_4$  elimination capacity at a constant methane loading rate ( $437(\pm 5.9) \text{ g m}^{-3} \text{ h}^{-1}$ ) in FBB and FB.

### 3.4 Influence of *n*-pentane on the $\text{CH}_4$ elimination capacity at a constant $\text{CH}_4$ loading rate

The addition of *n*-pentane aimed at providing an alternative carbon source to methane in order to foster the growth of *Fusarium solani* and to increase its surface hydrophobicity according to Vergara-Fernández et al. [8]. An increase in the  $\text{CH}_4$  EC was observed in both biofilters when the *n*-pentane loading rate increased at a constant methane loading rate of  $60 \text{ g m}^{-3} \text{ h}^{-1}$  (Figure 5). This increase was likely due to the higher hydrophobicity degree of the fungal cell wall, which mediated higher mass transfer rates and bioavailability of  $\text{CH}_4$  for the fungal and fungal-bacterial biomass. While  $\text{CH}_4$  EC in both biofilters was approximately  $12 \text{ g m}^{-3} \text{ h}^{-1}$  at a methane loading rate of  $60 \text{ g m}^{-3} \text{ h}^{-1}$ , the supplementation of *n*-pentane at  $107 \text{ g m}^{-3} \text{ h}^{-1}$  at a similar methane loading rate increased the EC of FB by 75% ( $21 \pm 1.0 \text{ g m}^{-3} \text{ h}^{-1}$ ) and by 34% in the FBB ( $16 \pm 1.1 \text{ g m}^{-3} \text{ h}^{-1}$ ). The higher

1  
2  
3  
4 increase of *EC* in FB during *n*-pentane supplementation could be explained by the increase in the  
5  
6 gas-biomass contact area mediated by the enhanced hyphae growth of the fungus in the presence  
7  
8 of a hydrophobic carbon source such as *n*-pentane (Vergara-Fernández et al., 2011).  
9



10  
11  
12  
13  
14  
15  
16  
17  
18  
19  
20  
21  
22  
23  
24  
25  
26  
27  
28  
29  
30  
31  
32  
33  
34 **Figure 5.** Influence of *n*-pentane loading rate on CH<sub>4</sub> elimination capacity in FBB and FB.  
35  
36  
37

### 38 3.5 Estimation of *Fusarium solani* contribution to CH<sub>4</sub> biodegradation

39  
40  
41 Figure 6 shows the results obtained for the biodegradation of methane in microcosm assays. When  
42  
43 amphotericin B was added to the packing material drawn from the FB (only *F. solani* was  
44  
45 inoculated), no biodegradation of CH<sub>4</sub> was observed (Figure 6a). In the control microcosm (without  
46  
47 amphotericin B) CH<sub>4</sub> degradation was observed at a rate of 0.9 g m<sup>-3</sup> d<sup>-1</sup>, indicating that *F. solani*  
48  
49 not only promotes the mass transfer of CH<sub>4</sub> to the biofilm but contributes to CH<sub>4</sub> biodegradation.  
50  
51 CH<sub>4</sub> biodegradation as the sole carbon and energy source by *Fusarium solani* was previously  
52  
53 observed by Vergara-Fernández et al. [11]. On the other hand, when amphotericin B was added to  
54  
55 the microcosms with *Fusarium solani* and methanotrophic bacteria, CH<sub>4</sub> biodegradation decreased  
56  
57  
58  
59  
60  
61  
62  
63  
64  
65

from  $1.3 \text{ g m}^{-3} \text{ d}^{-1}$  to  $0.6 \text{ g m}^{-3} \text{ d}^{-1}$  (Figure 6b). This finding confirmed the beneficial effect of using a fungal/bacterial consortium for the biodegradation of  $\text{CH}_4$ . The methanotrophic bacterial consortium was able to biodegrade 46% of the initial  $\text{CH}_4$ , while fungi biodegraded 54%.

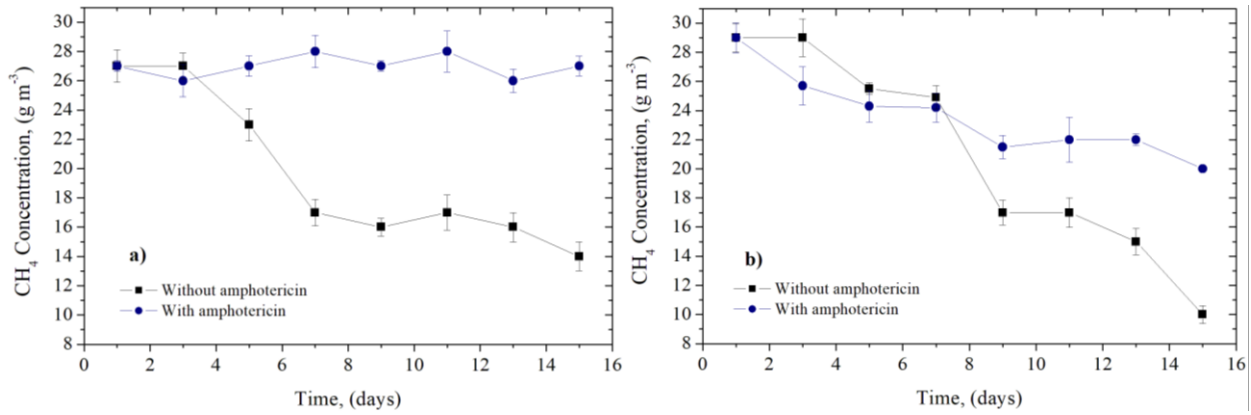


**Figure 6.** Effect of the addition of amphotericin B on the biodegradation of  $\text{CH}_4$  in biomass obtained from a) the fungal biofilter, b) from the fungal/bacterial biofilter.

### 3.6 Characterization of the rate-limiting step: $K_{BA}$ , biokinetics parameters and second Damköhler number estimation

Six dedicated experiments (three for the fungal and three for the fungal-bacterial biofilter) in duplicate were performed for the estimation of the global volumetric mass-transfer coefficient based on the biofilm phase ( $K_B a$ ). The model coupling external mass transfer and bioreaction in the biofilter (Eqs. S1 to S3) was calibrated to the fungal and the fungal-bacterial biofilters  $\text{CH}_4$  concentrations time-dependent data presented in Figure 7 and the steady-state  $\text{CH}_4$  EC data presented in Figure 3.

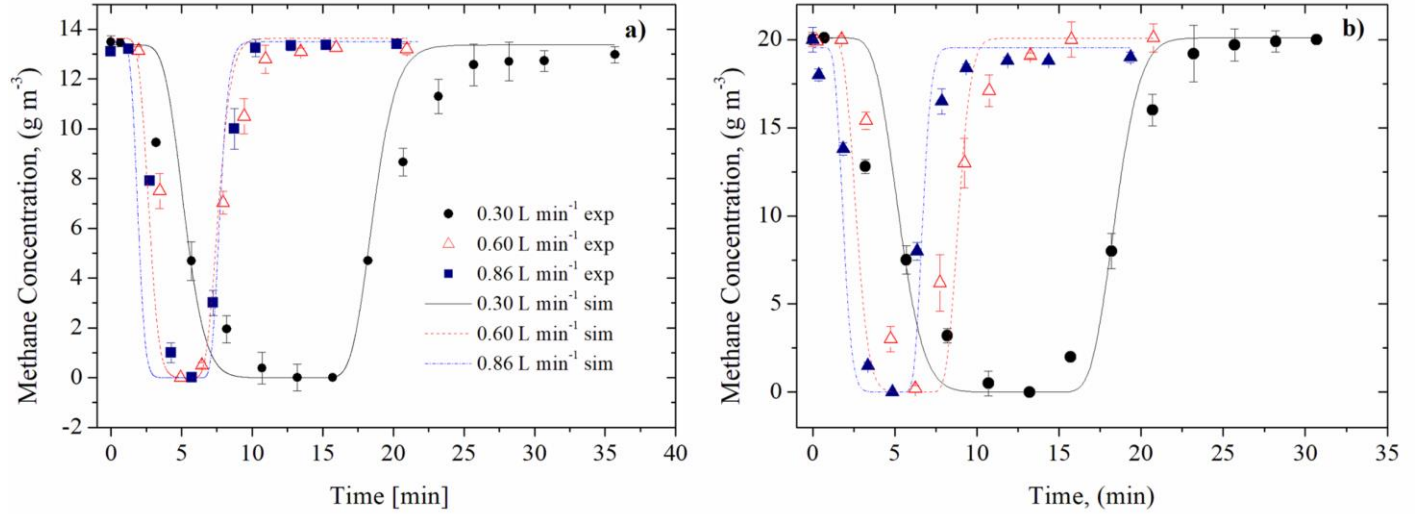


**Figure 7.** Dynamic CH<sub>4</sub>-in/CH<sub>4</sub> out experiments for the estimation of  $K_L a$  in a) FB and b) FBB.

The fitted parameters are shown in Table 1. The biofilm volume ( $V_b$ ) in each biofilter was estimated based on the experimental biomass content and the dimensions of the packing material. The dry weight (ash-free) biomass content per mass of dry vermiculite was quantified as  $102 \pm 15 \text{ mg}_{biomass} \text{ g}^{-1}$  in FB and  $99 \pm 16 \text{ mg}_{biomass} \text{ g}^{-1}$  in FBB. Assuming a biofilm density of  $1000 \text{ kg m}^{-3}$ , this is equivalent to a biofilm volume ( $V_b$ ) of  $8.4 \cdot 10^{-6} \text{ m}^3$  and  $8.1 \cdot 10^{-6} \text{ m}^3$  for the FB and FBB, respectively. To ensure the feasibility of these values, biofilm depth was estimated by measuring the dimensions of 57 random vermiculite particles and estimating their volume as a parallelepiped. Assuming a biofilm density of  $1000 \text{ kg m}^{-3}$ , the required biofilm depth to achieve the measured biomass contents per mass of vermiculite were  $25.5 \text{ }\mu\text{m}$  and  $24.5 \text{ }\mu\text{m}$  for FB and FBB, respectively. These biofilm thicknesses were comparable to the  $40 \text{ }\mu\text{m}$  measured in a bacterial biofilm of a biofilter degrading a mixture of benzene and toluene [33], but were smaller than the  $240\text{-}280 \text{ }\mu\text{m}$  reported by Cox *et al.* [34] for the biofilm formed in a biofilter degrading styrene (a less hydrophobic compound compared to CH<sub>4</sub>).

1  
2  
3  
4  $K_B a$  values for each biofilter were directly proportional to the inlet air flow rate, with coefficients  
5  
6 of determination of 0.997 and 0.954 for the FB and FBB, respectively. Despite data of global mass  
7  
8 transfer coefficients for biofilters are scarce in the literature, the estimated  $K_B a$  values compared  
9  
10 well with the values found by Nielsen *et al.* [35] for toluene biofiltration using lightweight  
11  
12 aggregates (Leca<sup>®</sup> pellets) as support with  $K_L a$  values ranging from 9.7 to 38.2 h<sup>-1</sup>. Considering  
13  
14 the aerial morphology of fungal hyphae compared to planar biofilms formed by bacteria (see Figure  
15  
16 S4 and S5), an increase in the specific area for mass transfer could be expected, an observation  
17  
18 previously reported in literature [9,30]. However, the mass transfer coefficients calculated in this  
19  
20 study revealed that the  $K_B a$  values of FB are smaller than those estimated for FBB. On the other  
21  
22 hand, *n*-pentane cofeeding experiments showed that CH<sub>4</sub> EC was improved by the presence of a  
23  
24 VOC known to increase the hydrophobicity of *F. solani* [36]. Moreover, the sensitivity analysis of  
25  
26 the values estimated for the model parameters (see Figures S2 and S3) indicated that, with the  
27  
28 exception of the  $K_B a$  values for steady state experiments, the sensitivity of the model towards the  
29  
30 mass transfer coefficient values was low. In brief, these findings highlight the key role of  
31  
32 hydrophobicity (decrease of the pollutant partition coefficient) over the potential enhancements of  
33  
34 the morphological structure of aerial hyphae in fungal-based biofilters.  
35  
36  
37  
38  
39  
40  
41  
42  
43  
44  
45  
46  
47  
48  
49  
50  
51  
52  
53  
54  
55  
56  
57  
58  
59  
60  
61  
62  
63  
64  
65

**Table 1.** Parameters obtained after calibrating the model of mass-transfer and reaction (Eqs. 4-6) using the experimental data presented in Figures 4 and 7.

Parameters	Units	Fungal biofilter (FB)	Fungal bacterial biofilter (FBB)
$K_B a_{0.3 \text{ LPM}}$	$h^{-1}$	2.5	8.5
$K_B a_{0.6 \text{ LPM}}$	$h^{-1}$	6.9	12.3
$K_B a_{0.86 \text{ LPM}}$	$h^{-1}$	10.2	19.1
$K_B a_{SS-0.19 \text{ LPM}}$	$h^{-1}$	0.6	2.7
$K_s$	$g \text{ CH}_4 m_{biomass}^{-3}$	0.3	-
$q_{max}$	$g \text{ CH}_4 g_{biomass}^{-1} h^{-1}$	4200	-
$k$	$m^3 g_{biomass}^{-1} h^{-1}$	-	914

Figure 8 shows the effect of the gas flow rate over the Damköhler number on FB and FBB. In FBB, the Damköhler number was independent of the inlet  $\text{CH}_4$  concentration as a result of the first-order kinetic assumption (see Eq. 7). However, the inlet  $\text{CH}_4$  concentration influenced the Damköhler number in FB and this effect is also shown in Figure 8. Interestingly, our calculations suggest that FBB was mass transfer limited regardless of the inlet flow tested, which agreed with observations reported in section 3.3. On the other hand, FB seems to be bioreaction limited except at low  $\text{CH}_4$  concentrations and low gas flow rates ( $0.19 \text{ L min}^{-1}$  equivalent to an EBRT of 12.4 min), an observation supported by the influence of EBRT on  $\text{CH}_4$  EC (see Section 3.3). Gomez- Borraz *et al.* [16] concluded that the performance of a compost bacteria-colonized biofilter was limited by the mass transport instead of by the bioreaction at a similar EBRT of 19 min and an inlet  $\text{CH}_4$  concentration of  $21 \text{ g m}^{-3}$ .

The sensitivity analysis of the model parameters over a wide range (0.5 to 1.5 times the optimal value) indicates that for the FBB the parameter with the highest sensitivity was  $K_B a_{SS-0.19 \text{ LPM}}$ , while the mass transfer coefficients for the experiments performed at higher gas velocities have little impact on model fit (see supplementary material, Figures S2 and S3). Interestingly, the model

fit showed little sensitivity towards the first-order reaction rate constant. A similar trend was found in FB, albeit in this case the model was found to be sensitive to the maximum specific uptake rate ( $q_{max}$ ) values. The sensitivity analysis confirmed the trends highlighted by the analysis of the Damköhler numbers.

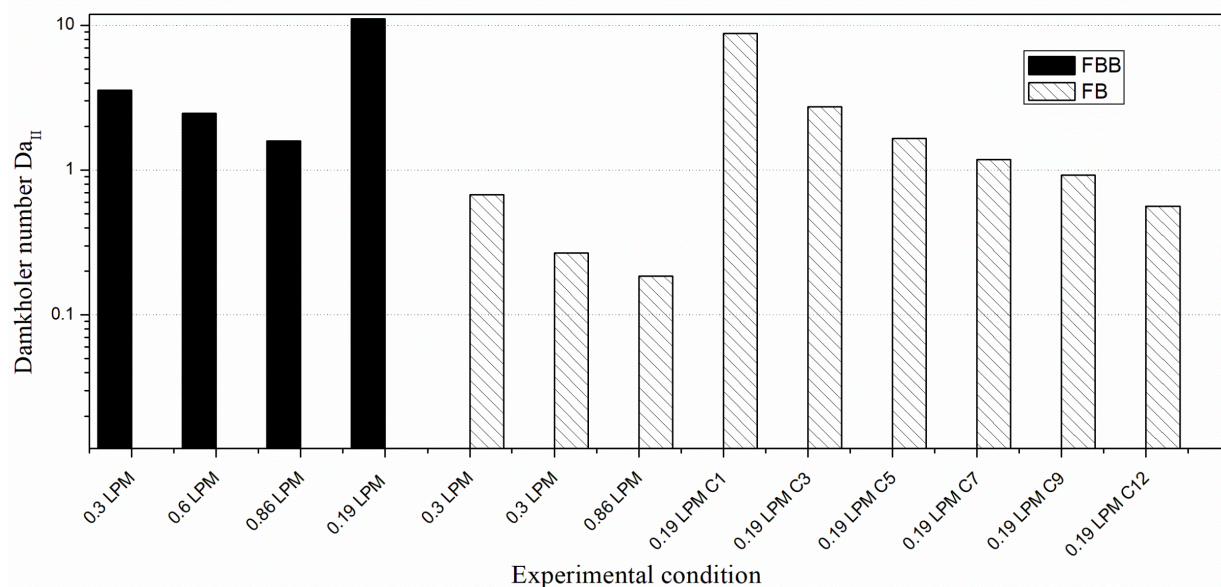


**Figure 8.** Estimated second Damköhler numbers at different inlet flow rates (logarithmic scale). For both biofilters, the flows 0.3, 0.6 and 0.86 L min<sup>-1</sup> corresponded to the dynamic assays (Figure 7). Values shown for 0.19 L min<sup>-1</sup> were obtained at steady-state under different inlet CH<sub>4</sub> concentrations (concentrations C1 to C12 in g m<sup>-3</sup>: 6, 19.2, 31.9, 44.6, 57.2, and 94.0).

#### 4 Conclusion

This work confirmed that the filamentous fungi *Fusarium solani* can degrade CH<sub>4</sub> as the sole carbon and energy source. The CH<sub>4</sub> elimination capacities of a biofilter inoculated with *F. solani* and bacterial methanotrophic consortium were higher than those recorded in a biofilter inoculated only with fungi regardless of the inlet loads and EBRTs tested, except when *n*-pentane was co-fed along with CH<sub>4</sub>. The exposure of the fungal biomass to *n*-pentane, a highly hydrophobic and easily

1  
2  
3  
4 degradable VOC, during CH<sub>4</sub> biofiltration further improved the CH<sub>4</sub> EC likely due to an increase  
5  
6 in the surface hydrophobicity and transport area of fungal hyphae. Overall, the fungal filter  
7  
8 performance was bioreaction limited, while mass transport limitations were encountered in the  
9  
10 fungal/bacterial biofilter. Finally, the estimated mass transfer coefficients and Damköhler numbers  
11  
12 suggest that the beneficial effect of *F. solani* during CH<sub>4</sub> biofiltration was mediated by biomass  
13  
14 hydrophobicity rather than to the formation of aerial hyphae structures increasing the mass transfer  
15  
16 area.  
17  
18  
19  
20  
21  
22

## 23 **5 Conflict of Interest**

24  
25 *The authors declare that the research was conducted in the absence of any commercial or financial*  
26  
27 *relationships that could be construed as a potential conflict of interest.*  
28  
29  
30  
31  
32

## 33 **6 Acknowledgments**

34  
35 The present work has been sponsored by the National Agency for Research and Development  
36  
37 (ANID Chile) (Fondecyt 1160220). F. Carreño, A. Vergara and F. Scott acknowledge financial  
38  
39 support from grant Apoyo a la Formación de Redes Internacionales entre Centros de Investigación  
40  
41 REDES190137, CONICYT-PCI. The financial support from the Regional Government of Castilla  
42  
43 y León and the EU-FEDER program (CLU 2017-09 and UIC 071) is also gratefully acknowledged.  
44  
45  
46  
47  
48

## 49 **7 References**

- 50  
51  
52 [1] T. Skytt, S.N. Nielsen, B.-G. Jonsson, Global warming potential and absolute global  
53  
54 temperature change potential from carbon dioxide and methane fluxes as indicators of  
55  
56 regional sustainability – A case study of Jämtland, Sweden, *Ecol. Indic.* 110 (2020) 105831.  
57  
58 doi:10.1016/j.ecolind.2019.105831.  
59  
60  
61  
62  
63  
64  
65

- 1  
2  
3  
4 [2] J. Nikiema, R. Brzezinski, M. Heitz, Elimination of methane generated from landfills by  
5 biofiltration: a review, *Rev. Environ. Sci. Bio/Technology*. 6 (2007) 261–284.  
6 doi:10.1007/s11157-006-9114-z.  
7  
8  
9  
10  
11 [3] J.C. López, G. Quijano, T.S.O. Souza, J.M. Estrada, R. Lebrero, R. Muñoz, Biotechnologies  
12 for greenhouse gases (CH<sub>4</sub>, N<sub>2</sub>O, and CO<sub>2</sub>) abatement: state of the art and challenges, *Appl.*  
13 *Microbiol. Biotechnol.* 97 (2013) 2277–2303. doi:10.1007/s00253-013-4734-z.  
14  
15  
16  
17  
18 [4] C. Du Plessis, J. Strauss, E. Sebapalo, K. Riedel, Empirical model for methane oxidation  
19 using a composted pine bark biofilter\*, *Fuel*. 82 (2003) 1359–1365. doi:10.1016/S0016-  
20 2361(03)00040-1.  
21  
22  
23  
24  
25 [5] M. Girard, A.A. Ramirez, G. Buelna, M. Heitz, Biofiltration of methane at low  
26 concentrations representative of the piggery industry—Influence of the methane and  
27 nitrogen concentrations, *Chem. Eng. J.* 168 (2011) 151–158. doi:10.1016/j.cej.2010.12.054.  
28  
29  
30  
31  
32 [6] S. Arriaga, S. Revah, Improving hexane removal by enhancing fungal development in a  
33 microbial consortium biofilter, *Biotechnol. Bioeng.* 90 (2005) 107–115.  
34 doi:10.1002/bit.20424.  
35  
36  
37  
38 [7] J.W. Van Groenestijn, J.X. Liu, Removal of alpha-pinene from gases using biofilters  
39 containing fungi, *Atmos. Environ.* 36 (2002) 5501–5508. doi:10.1016/S1352-  
40 2310(02)00665-9.  
41  
42  
43  
44  
45 [8] A. Vergara-Fernández, B. Van Haaren, S. Revah, Phase partition of gaseous hexane and  
46 surface hydrophobicity of *Fusarium solani* when grown in liquid and solid media with  
47 hexanol and hexane, *Biotechnol. Lett.* 28 (2006). doi:10.1007/s10529-006-9186-4.  
48  
49  
50  
51 [9] A. Vergara-Fernández, S. Hernández, S. Revah, Phenomenological model of fungal  
52 biofilters for the abatement of hydrophobic VOCs, *Biotechnol. Bioeng.* 101 (2008) 1182–  
53 1192. doi:10.1002/bit.21989.  
54  
55  
56  
57  
58  
59  
60  
61  
62  
63  
64  
65

- 1  
2  
3  
4 [10] R. Muñoz, S. Villaverde, B. Guieysse, S. Revah, Two-phase partitioning bioreactors for  
5 treatment of volatile organic compounds, *Biotechnol. Adv.* 25 (2007) 410–422.  
6 doi:10.1016/j.biotechadv.2007.03.005.  
7  
8  
9  
10  
11 [11] A. Vergara-Fernández, P. Morales, F. Scott, S. Guerrero, L. Yañez, S. Mau, G. Aroca,  
12 Methane biodegradation and enhanced methane solubilization by the filamentous fungi  
13 *Fusarium solani.*, *Chemosphere.* 226 (2019) 24–35.  
14 doi:10.1016/j.chemosphere.2019.03.116.  
15  
16  
17  
18  
19  
20  
21 [12] M. Girard, P. Viens, A.A. Ramirez, R. Brzezinski, G. Buelna, M. Heitz, Simultaneous  
22 treatment of methane and swine slurry by biofiltration, *J. Chem. Technol. Biotechnol.* 87  
23 (2012) 697–704. doi:10.1002/jctb.3692.  
24  
25  
26  
27  
28  
29 [13] R. Lebrero, J.C. López, I. Lehtinen, R. Pérez, G. Quijano, R. Muñoz, Exploring the potential  
30 of fungi for methane abatement: Performance evaluation of a fungal-bacterial biofilter,  
31 *Chemosphere.* 144 (2016) 97–106. doi:10.1016/j.chemosphere.2015.08.017.  
32  
33  
34  
35  
36 [14] J.P. Oliver, J.S. Schilling, Capture of methane by fungi: evidence from laboratory-scale  
37 biofilter and chromatographic isotherm studies, *Trans. ASABE.* 59 (2016) 1791–1801.  
38 doi:10.13031/trans.59.11595.  
39  
40  
41  
42  
43 [15] V.B. Stein, J.P. Hettiaratchi, Methane oxidation in three Alberta soils: influence of soil  
44 parameters and methane flux rates., *Environ. Technol.* 22 (2001) 101–11.  
45 doi:10.1080/09593332208618315.  
46  
47  
48  
49  
50 [16] T.L. Gómez-Borraz, A. González-Sánchez, W. Bonilla-Blancas, S. Revah, A. Noyola,  
51 Characterization of the biofiltration of methane emissions from municipal anaerobic  
52 effluents, *Process Biochem.* 63 (2017) 204–213. doi:10.1016/j.procbio.2017.08.011.  
53  
54  
55  
56  
57 [17] V.C. Hettiarachchi, J.P.A. Hettiaratchi, A.K. Mehrotra, Comprehensive One-Dimensional  
58 Mathematical Model for Heat, Gas, and Moisture Transport in Methane Biofilters, *Pract.*  
59  
60  
61  
62  
63  
64  
65

- 1  
2  
3  
4 Period. Hazardous, Toxic, Radioact. Waste Manag. 11 (2007) 225–233.  
5  
6 doi:10.1061/(ASCE)1090-025X(2007)11:4(225).  
7  
8
- [18] M. Cáceres, J.C. Gentina, G. Aroca, Oxidation of methane by *Methylobacterium album*  
9 and *Methylocystis* sp. in the presence of H<sub>2</sub>S and NH<sub>3</sub>, *Biotechnol. Lett.* 36 (2014) 69–74.  
10  
11 doi:10.1007/s10529-013-1339-7.  
12  
13
- [19] P. Morales, M. Cáceres, F. Scott, L. Díaz-Robles, G. Aroca, A. Vergara-Fernández,  
14  
15  
16  
17  
18  
19  
20  
21  
22  
23  
24  
25  
26  
27  
28  
29  
30  
31  
32  
33  
34  
35  
36  
37  
38  
39  
40  
41  
42  
43  
44  
45  
46  
47  
48  
49  
50  
51  
52  
53  
54  
55  
56  
57  
58  
59  
60  
61  
62  
63  
64  
65
- [20] E.I. García-Peña, S. Hernández, E. Favela-Torres, R. Auria, S. Revah, Toluene biofiltration  
by the fungus *Scedosporium apiospermum* TB1, *Biotechnol. Bioeng.* 76 (2001) 61–69.  
doi:10.1002/bit.1026.
- [21] S. Arriaga, S. Revah, Removal of n-hexane by *Fusarium solani* with a gas-phase biofilter, *J.*  
*Ind. Microbiol. Biotechnol.* 32 (2005) 548–553. doi:10.1007/s10295-005-0247-9.
- [22] M. Cáceres, A.D. Dorado, J.C. Gentina, G. Aroca, Oxidation of methane in biotrickling  
filters inoculated with methanotrophic bacteria, *Environ. Sci. Pollut. Res.* 24 (2017) 25702–  
25712. doi:10.1007/s11356-016-7133-z.
- [23] A. Vergara-Fernández, S. Hernández, S. Revah, Elimination of hydrophobic volatile organic  
compounds in fungal biofilters: Reducing start-up time using different carbon sources,  
*Biotechnol. Bioeng.* 108 (2011). doi:10.1002/bit.23003.
- [24] T. Van Daele, D. Fernandes del Pozo, D. Van Hauwermeiren, K. V. Gernaey, R.  
Wohlgemuth, I. Nopens, A generic model-based methodology for quantification of mass  
transfer limitations in microreactors, *Chem. Eng. J.* 300 (2016) 193–208.  
doi:10.1016/j.cej.2016.04.117.

- 1  
2  
3  
4 [25] M.A. Deshusses, G. Hamer, I.J. Dunn, Behavior of Biofilters for Waste Air Biotreatment.  
5  
6 1. Dynamic Model Development, Environ. Sci. Technol. 29 (1995) 1048–1058.  
7  
8 doi:10.1021/es00004a027.  
9  
10  
11 [26] K.D. Kits, M.G. Kalyuzhnaya, M.G. Klotz, M.S.M. Jetten, H.J.M. Op den Camp, S.  
12  
13 Vuilleumier, F. Bringel, A.A. DiSpirito, J.C. Murrell, D. Bruce, J.-F. Cheng, A. Copeland,  
14  
15 L. Goodwin, L. Hauser, A. Lajus, M.L. Land, A. Lapidus, S. Lucas, C. Medigue, S. Pitluck,  
16  
17 T. Woyke, A. Zeytun, L.Y. Stein, Genome Sequence of the Obligate Gammaproteobacterial  
18  
19 Methanotroph *Methylomicrobium album* Strain BG8, Genome Announc. 1 (2013).  
20  
21 doi:10.1128/genomeA.00170-13.  
22  
23  
24 [27] A. Vorobev, S. Jagadevan, S. Jain, K. Anantharaman, G.J. Dick, S. Vuilleumier, J.D.  
25  
26 Semrau, Genomic and Transcriptomic Analyses of the Facultative Methanotroph  
27  
28 *Methylocystis* sp. Strain SB2 Grown on Methane or Ethanol, Appl. Environ. Microbiol. 80  
29  
30 (2014) 3044–3052. doi:10.1128/AEM.00218-14.  
31  
32  
33 [28] C. Pratt, A.S. Walcroft, K.R. Tate, D.J. Ross, R. Roy, M.H. Reid, P.W. Veiga, Biofiltration  
34  
35 of methane emissions from a dairy farm effluent pond, Agric. Ecosyst. Environ. 152 (2012)  
36  
37 33–39. doi:10.1016/j.agee.2012.02.011.  
38  
39  
40 [29] J.C. López, L. Merchán, R. Lebrero, R. Muñoz, Feast-famine biofilter operation for methane  
41  
42 mitigation, J. Clean. Prod. 170 (2018) 108–118. doi:10.1016/j.jclepro.2017.09.157.  
43  
44  
45 [30] A. Vergara-Fernández, F. Scott, P. Moreno-Casas, L. Díaz-Robles, R. Muñoz, L. Diaz-  
46  
47 Robles, R. Muñoz, L. Díaz-Robles, R. Muñoz, Elucidating the key role of the fungal  
48  
49 mycelium on the biodegradation of n-pentane as a model hydrophobic VOC, Chemosphere.  
50  
51 157 (2016) 89–96. doi:10.1016/j.chemosphere.2016.05.034.  
52  
53  
54 [31] A. Vergara-Fernández, B. Van Haaren, S. Revah, Phase partition of gaseous hexane and  
55  
56 surface hydrophobicity of *Fusarium solani* when grown in liquid and solid media with  
57  
58  
59  
60  
61  
62  
63  
64  
65

1  
2  
3  
4 hexanol and hexane, *Biotechnol. Lett.* 28 (2006) 2011–2017. doi:10.1007/s10529-006-  
5  
6 9186-4.

7  
8  
9 [32] A. Vergara-Fernández, S. Hernández, J. San Martín-Davison, S. Revah, Morphological  
10 characterization of aerial hyphae and simulation growth of *Fusarium solani* under different  
11 carbon source for application in the hydrophobic VOCs biofiltration, *Rev. Mex. Ing.*  
12 *Química.* 10 (2011) 225–233.

13  
14  
15  
16  
17 [33] S.M. Zarook, A.A. Shaikh, Z. Ansar, B.C. Baltzis, Biofiltration of volatile organic  
18 compound (VOC) mixtures under transient conditions, *Chem. Eng. Sci.* 52 (1997) 4135–  
19 4142. doi:10.1016/S0009-2509(97)00256-X.

20  
21  
22  
23  
24 [34] H.H.J. Cox, R.E. Moerman, S. van Baalen, W.N.M. van Heiningen, H.J. Doddema, W.  
25 Harder, Performance of a styrene-degrading biofilter containing the yeast *Exophiala*  
26 *jeanselmei*, *Biotechnol. Bioeng.* 53 (1997) 259–266. doi:10.1002/(SICI)1097-  
27 0290(19970205)53:3<259::AID-BIT3>3.0.CO;2-H.

28  
29  
30  
31  
32 [35] A.M. Nielsen, L.P. Nielsen, A. Feilberg, K.V. Christensen, A Method for Estimating Mass-  
33 Transfer Coefficients in a Biofilter from Membrane Inlet Mass Spectrometer Data, *J. Air*  
34 *Waste Manage. Assoc.* 59 (2009) 155–162. doi:10.3155/1047-3289.59.2.155.

35  
36  
37  
38  
39 [36] A. Vergara-Fernández, O. Soto-Sánchez, J. Vásquez, A. Vergara-Fernandez, O. Soto-  
40 Sanchez, J. Vasquez, A. Vergara-Fernández, O. Soto-Sánchez, J. Vásquez, O. Soto-Sanchez,  
41 J. Vásquez-Bestagno, A. Vergara-Fernandez, O. Soto-Sanchez, J. Vasquez, Effects of  
42 Packing Material Type on n-Pentane/Biomass Partition Coefficient for Use in Fungal  
43 Biofilters, *Chem. Biochem. Eng. Q.* 25 (2011) 439–444.

44  
45  
46  
47  
48 Myhre, G., D. Shindell, F.-M. Bréon, W. Collins, J. Fuglestedt, J. Huang, D. Koch, J.-F.

49  
50  
51  
52  
53 Lamarque, D. Lee, B. Mendoza, T. Nakajima, A. Robock, G. Stephens, T. Takemura and H.

54  
55  
56  
57  
58 Zhang, 2013: Anthropogenic and Natural Radiative Forcing. In: *Climate Change 2013: The*

1  
2  
3  
4  
5  
6  
7  
8  
9  
10  
11  
12  
13  
14  
15  
16  
17  
18  
19  
20  
21  
22  
23  
24  
25  
26  
27  
28  
29  
30  
31  
32  
33  
34  
35  
36  
37  
38  
39  
40  
41  
42  
43  
44  
45  
46  
47  
48  
49  
50  
51  
52  
53  
54  
55  
56  
57  
58  
59  
60  
61  
62  
63  
64  
65

Physical Science Basis. Contribution of Working Group I to the Fifth Assessment Report of the Intergovernmental Panel on Climate Change [Stocker, T.F., D. Qin, G.-K. Plattner, M. Tignor, S.K. Allen, J. Boschung, A. Nauels, Y. Xia, V. Bex and P.M. Midgley (eds.)]. Cambridge University Press, Cambridge, United Kingdom and New York, NY, USA.

Stein, V.B., Hettiaratchi, J.P., 2001. Methane oxidation in three Alberta soils: influence of soil parameters and methane flux rates. *Environ. Technol.* 22, 101–11. doi:10.1080/09593332208618315

1  
2  
3  
4  
5  
6  
7  
8  
9  
10  
11  
12  
13  
14  
15  
16  
17  
18  
19  
20  
21  
22  
23  
24  
25  
26  
27  
28  
29  
30  
31  
32  
33  
34  
35  
36  
37  
38  
39  
40  
41  
42  
43  
44  
45  
46  
47  
48  
49  
50  
51  
52  
53  
54  
55  
56  
57  
58  
59  
60  
61  
62  
63  
64  
65

## Supporting Information

# A comparative assesement of the performance of fungal-bacterial and fungal biofilters for methane abatement

Alberto Vergara-Fernández<sup>1\*</sup>, Felipe Scott<sup>1</sup>, Felipe Carreño<sup>1</sup>, Germán Aroca<sup>2</sup>, Patricio Moreno-Casas<sup>1</sup>, Armando González-Sánchez<sup>4</sup> and Raúl Muñoz<sup>3</sup>

A simplified version of the mathematical model of a biofilter proposed by Deshusses et al. [25] was applied for the estimation of the global volumetric mass transfer coefficient ( $K_{Ba}$ ). In the original work of Deshusses et al. [25], the gas phase in a biofilter was modeled as a cascade of stirred tank reactors (STRs). In the present work, each STR containing gas phase was connected not only to the previous and the following gas-phase STR, but also to the a STR representing the biofilm where bioreactions occur (see Figure S1). The super-script  $j$  stands for each biofilter.

### Assumptions:

- Each subdivision of the gas-phase and the biofilm-phase is ideally mixed.
- The  $i$ -th gas phase STR has a volume equal to  $\epsilon V_p/N$ , where  $N$  is the number of reactors along the height of biofilter.
- The  $i$ -th layer is fed from the  $i-1$  stage at a rate  $QG_{i-1}^j$  and the methane mass flow exiting this stage is  $QG_i^j$ .

- Methane from the  $i$ -th gas-phase stage is transferred to the  $i$ -th biofilm phase at a rate  $J_i = \frac{K_B a (1-\epsilon) V_p}{N} \left( \frac{G_i^j}{H} - B_i^j \right)$ , where  $B_i^j$  is the dissolved methane concentration in the  $i$ -th layer of the  $j$ -th biofilter.
- Equilibrium and non-accumulation are assumed at the interface, hence the  $J_i$  is also the rate at which methane enters to the  $i$ -th biofilm section with volume  $V_b/N$ .
- In each section of the biofilm, no net growth of biomass is assumed during the experiments used for model calibration. Therefore, the biomass concentration  $X_b^j$  is constant and experimentally assessed. This assumption is justified since  $K_{La}$  estimation experiments and inlet load effect experiments (Figures 4 and 8) lasted three weeks.
- Moreover, it is assumed that the biocatalyst is homogeneously distributed throughout the biofilm.
- Finally, based on the results obtained in the experiments where inlet-load was changed, a first-order reaction kinetic was assumed to represent the activity of the biocatalyst in the biofilm for FBB and a Monod type kinetic for FB.

$$Q_s^j(C_b) = \begin{cases} kX_b^j B_j, & \text{for } j = \text{FBB} \\ q_{\max} X_b^j \frac{B^j}{K_s + B^j}, & \text{for } j = \text{FB} \end{cases} \quad \text{Eq. S1}$$

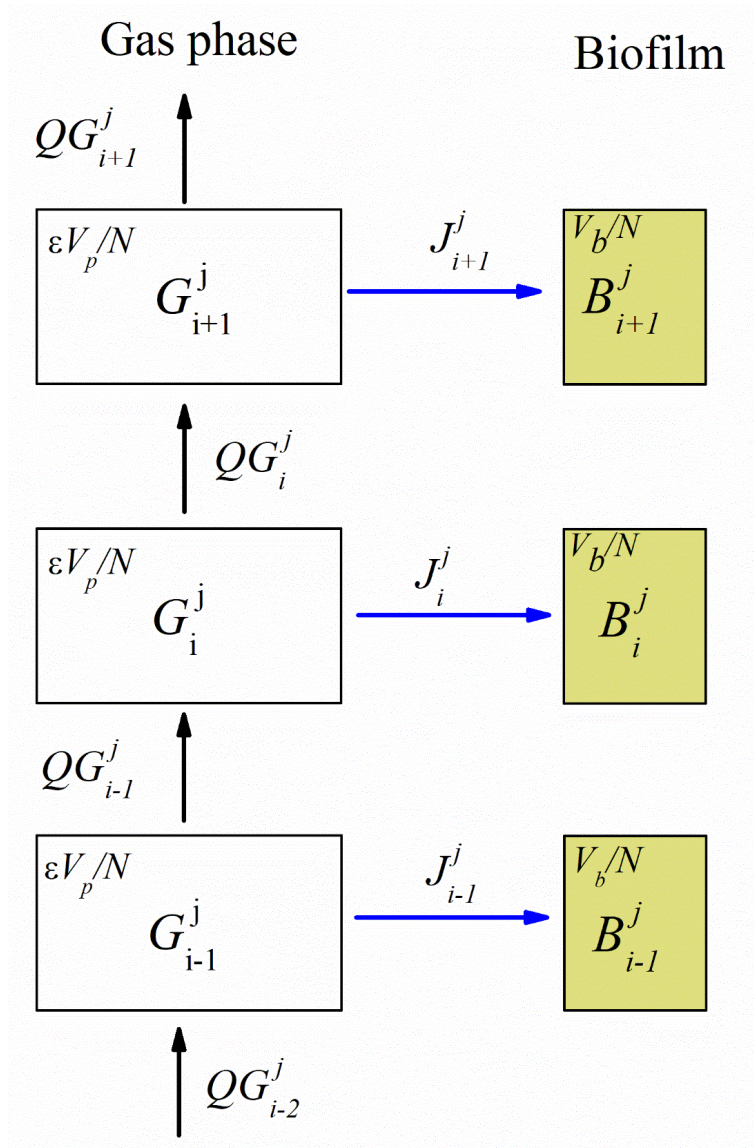


**Figure S1.** Schematic description of the mathematical model for one section of the biofilter. The  $\text{CH}_4$  laden air flows through the gas phase and  $\text{CH}_4$  is transferred from each subdivision of the gas phase to its corresponding section of the biofilm.

The acronym  $\varepsilon$  represents the empty fraction of the bed,  $A_T$  the cross-section of the reactor,  $Q$  the gas flow,  $K_B^j$  the global volumetric mass transfer coefficient based on the volume of biofilm and  $H_j$  the air-biofilm methane partition coefficient. The partition coefficient for the fungal biomass was

1  
2  
3  
4 directly taken from a previous work by the authors [11], while the partition coefficient for the fungal-  
5  
6 bacterial biofilms was estimated as 0.46 times the partition coefficient of the bacterial biomass and  
7  
8 0.64 times the partition coefficient of the fungal biomass. The factors 0.46 and 0.64 correspond to  
9  
10 the contributions of bacteria and fungi towards methane degradation in the microcosms inoculated  
11  
12 with biomass withdrawn from the FBB (see Section 2.6).  
13  
14

15  
16 A non-steady state methane mass balance to the gas phase leads to (Eq. 5).  
17

$$18 \frac{dG_i^j}{dt} = \frac{Q \cdot N}{\epsilon \cdot A_T \cdot L} [G_{i-1}^j(t) - G_i^j(t)] - K_B a^j \frac{(1-\epsilon)}{\epsilon} \left( \frac{G_i^j(t)}{H^j} - B_i^j(t) \right) \quad \text{Eq. S2}$$

19  
20  
21 With boundary conditions:  
22

$$23 G_i^j(0) = 0 \text{ for } i = \{1, \dots, N\} \text{ (empty initial reactor)}$$

$$24 G_i^j(t) = \begin{cases} G^{in} \text{ (feed concentration during steady state)} \\ 0 \text{ (during kLa experiments when methane flow is off)} \end{cases}$$

25  
26  
27  
28  
29  
30  
31  
32  
33 A methane balance to the i-th section of the homogenous biomass phase yields:  
34

$$35 \frac{dB_i^j}{dt} = K_B a^j (1 - \epsilon) \frac{V_R}{V_b^j} \left( \frac{G_i^j(t)}{H^j} - B_i^j(t) \right) - Q_s^j(B_i^j) \quad \text{Eq. S3}$$

36  
37  
38  
39  
40 The initial condition for this equation is either  $B_i(0) = 0$ , for all sections (empty reactor), or the  
41  
42 steady-state concentration per stage calculated using the operating conditions. The model  
43  
44 parameters  $K_B a^j$  value is dependent on the gas flow velocity. Therefore, a unique set of biokinetic  
45  
46 parameters  $k$ ,  $K_s$  and  $q_{max}$  was estimated for all the experiments, but eight values of  $K_B a$  were fitted  
47  
48 to account for the different gas flow rates (see Table 1). Parameters were estimated using non-linear  
49  
50 fitting (patternsearch, MATLAB®). The steady-state simulations were obtained by dropping the  
51  
52 differential terms in Eqs. (S2) and (S3).  
53  
54  
55  
56  
57  
58  
59  
60  
61  
62  
63  
64  
65

## Sensitivity analysis

Model fit was sensibilized for each parameter in an interval where the minimum value was 50% of the best fit of a parameter and the maximum value was 1.5 fold. The sensitivity analysis was carried out by varying two parameters at a time, one of the parameters being the maximum substrate uptake rate ( $q_{max}$ ) for the fungal biofilter or the first order coefficient for the fungal-bacterial biofilter ( $k$ ). The second parameter was a mass transfer coefficient. A full factorial approach was used, thereby each response surface is formed by 100 combinations were the average distance between the predicted and experimental values was calculated. The average distance was defined as  $\frac{\sqrt{SSE^j}}{N_m^j}$ , where  $SSE = (\epsilon^j)^T \epsilon^j$  was the sum of the squared error and was calculated as the product of the vector  $\epsilon^j = G_m^j - G_{out}^{j,*}$ , where  $G_m^j$  was the vector of the measured methane concentrations in the outlet of each biofilter  $j$  and  $G_{out}^{j,*}$  the vector of methane concentration predicted by the model for the optimal set of estimated parameters. Finally,  $N_m^j$  denoted the number of experimental measurements used for each biofilter.

1  
2  
3  
4  
5  
6  
7  
8  
9  
10  
11  
12  
13  
14  
15  
16  
17  
18  
19  
20  
21  
22  
23  
24  
25  
26  
27  
28  
29  
30  
31  
32  
33  
34  
35  
36  
37  
38  
39  
40  
41  
42  
43  
44  
45  
46  
47  
48  
49  
50  
51  
52  
53  
54  
55  
56  
57  
58  
59  
60  
61  
62  
63  
64  
65

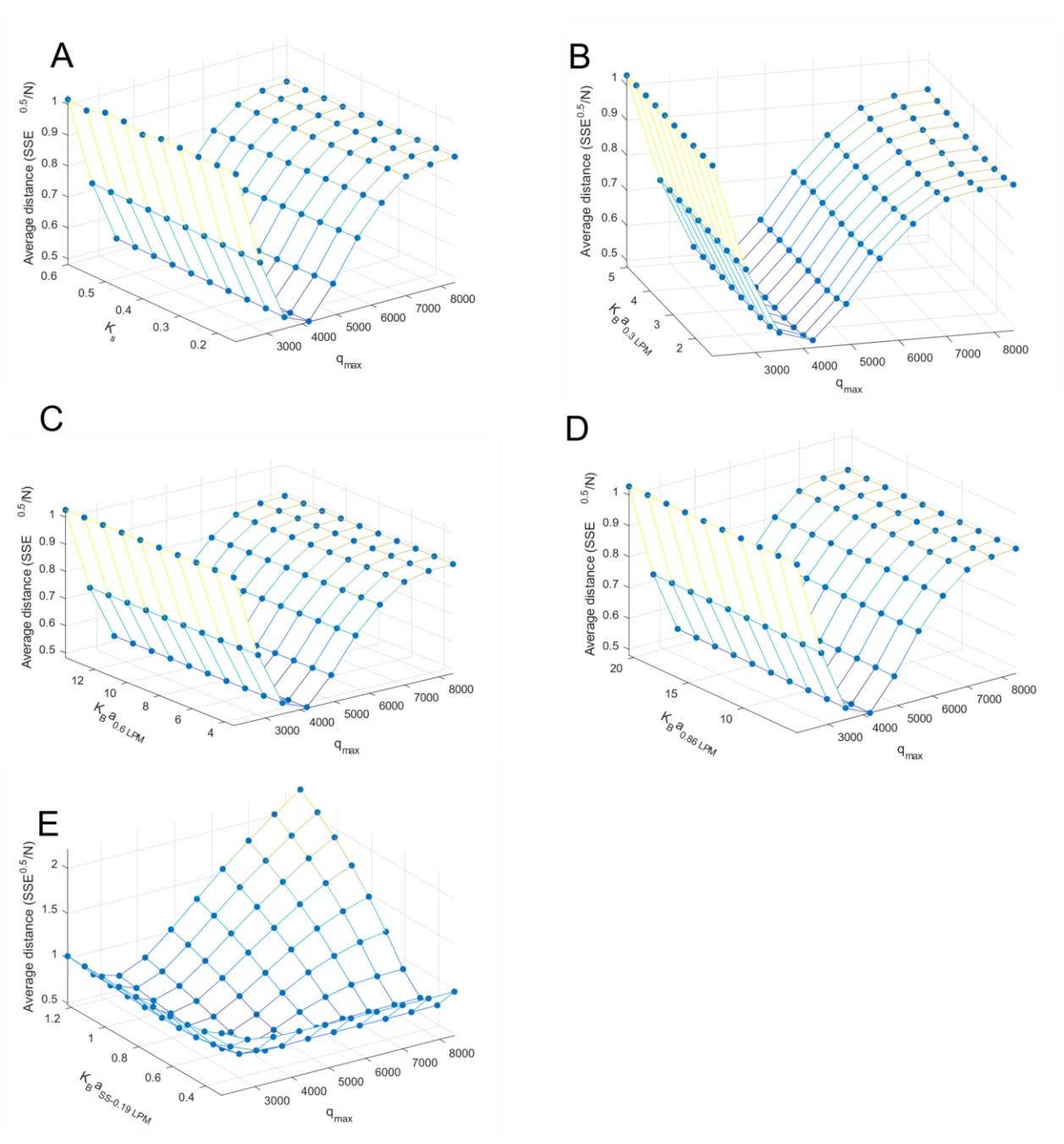
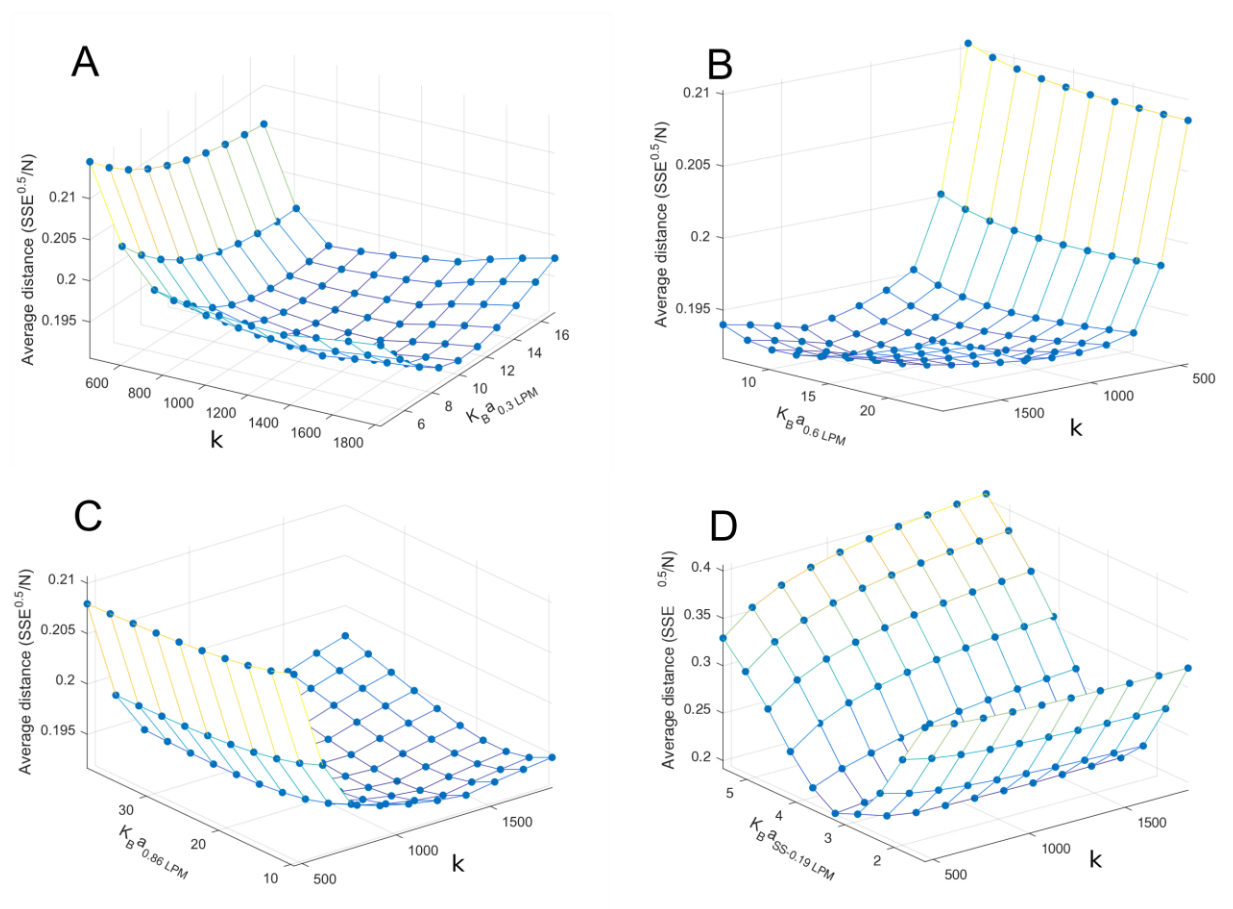


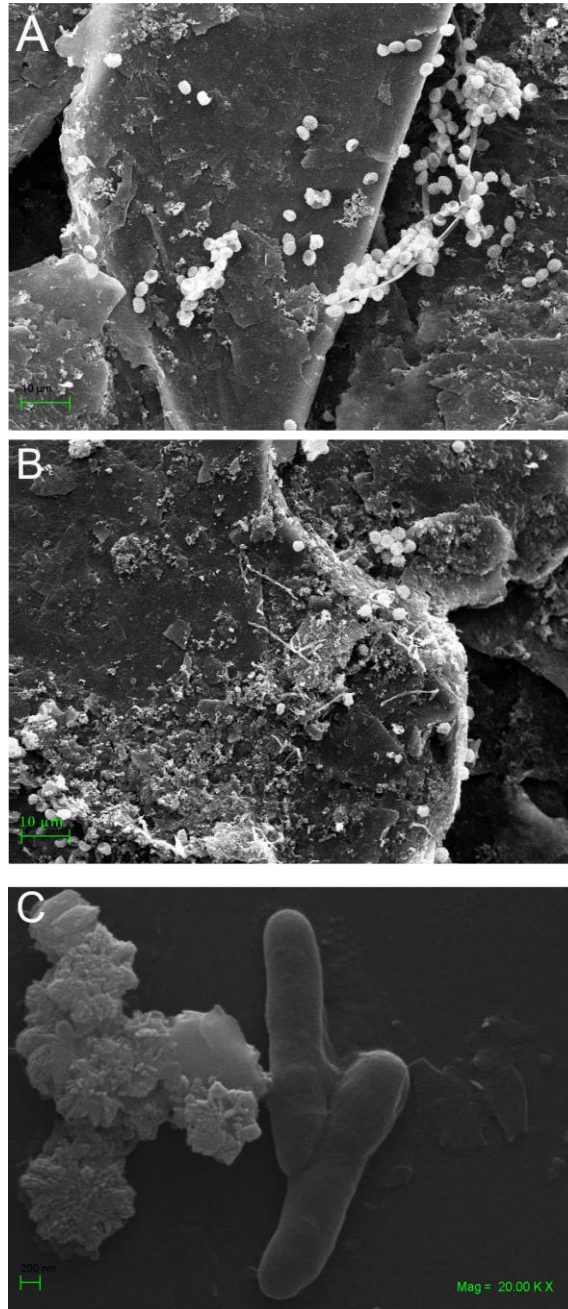
Figure S2. Sensitivity analysis of the optimal parameter values estimated for the FB..

1  
2  
3  
4  
5  
6  
7  
8  
9  
10  
11  
12  
13  
14  
15  
16  
17  
18  
19  
20  
21  
22  
23  
24  
25  
26  
27  
28  
29  
30  
31  
32  
33  
34  
35  
36  
37  
38  
39  
40  
41  
42  
43  
44  
45  
46  
47  
48  
49  
50  
51  
52  
53  
54  
55  
56  
57  
58  
59  
60  
61  
62  
63  
64  
65



**Figure S3.** Sensitivity analysis of the optimal parameter values estimated for FBB.

1  
2  
3  
4 **Scanning electron microscopy.**  
5  
6  
7



52 **Figure S4.** Scanning electron microscopy of the packing material withdrawn from the fungal-  
53 bacterial biofilter. The scale bar of A and B is 10 μm, C is 200 nm. Photographs A and B show the  
54 characteristic chlamydo-spores of *F. solani*. Photograph C shows two macroconidia next to what  
55 appears to be a crystal.  
56  
57  
58  
59  
60  
61  
62  
63  
64  
65

1  
2  
3  
4  
5  
6  
7  
8  
9  
10  
11  
12  
13  
14  
15  
16  
17  
18  
19  
20  
21  
22  
23  
24  
25  
26  
27  
28  
29  
30  
31  
32  
33  
34  
35  
36  
37  
38  
39  
40  
41  
42  
43  
44  
45  
46  
47  
48  
49  
50  
51  
52  
53  
54  
55  
56  
57  
58  
59  
60  
61  
62  
63  
64  
65

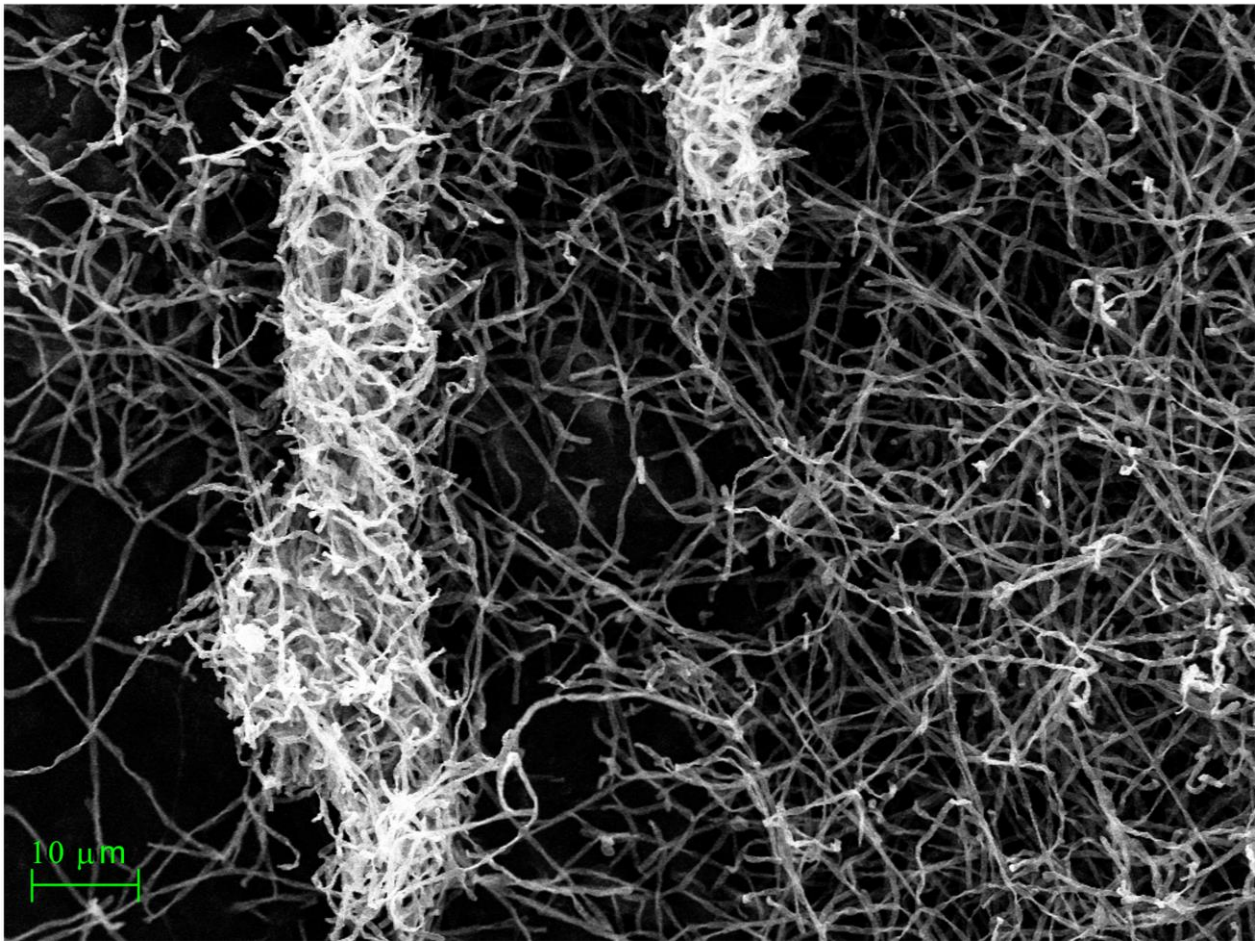


**Figure S5.** Scanning electron microscopy of the packing material withdrawn from the fungal biofilter. The scale bar is 10  $\mu\text{m}$ . The image shows the characteristic hyphae and microconidia of *F. solani*.

**Conflict of interest declaration for:**

*A comparative assessment of the performance of fungal-bacterial and fungal biofilters for methane abatement*

Alberto Vergara-Fernández, Felipe Scott, Felipe Carreño, Germán Aroca, Patricio Moreno-Casas, Armando González-Sánchez and Raúl Muñoz

The authors declare that the research was conducted in the absence of any commercial or financial relationships that could be construed as a potential conflict of interest.